

## 23. INFLATION

Written May 2016 by J. Ellis (King’s College London; CERN) and D. Wands (U. of Portsmouth).

### 23.1. Motivation and Introduction

The standard Big-Bang model of cosmology provides a successful framework in which to understand the thermal history of our Universe and the growth of cosmic structure, but it is essentially incomplete. As described in Sec. 22.2.4 in “Big Bang Cosmology” review, Big-Bang cosmology requires very specific initial conditions. It postulates a uniform cosmological background, described by a spatially-flat, homogeneous and isotropic Robertson-Walker (RW) metric (Eq. (22.1) in “Big Bang Cosmology” review), with scale factor  $R(t)$ . Within this setting, it also requires an initial almost scale-invariant distribution of primordial density perturbations as seen, for example, in the cosmic microwave background (CMB) radiation (described in Chap. 28, “Cosmic Microwave Background” review), on scales far larger than the causal horizon at the time the CMB photons last scattered.

The Hubble expansion rate,  $H \equiv \dot{R}/R$ , in a Robertson-Walker cosmology is given by the Friedmann constraint equation (Eq. (22.8) in “Big Bang Cosmology” review)

$$H^2 = \frac{8\pi\rho}{3M_P^2} + \frac{\Lambda}{3} - \frac{k}{R^2}, \quad (23.1)$$

where  $k/R^2$  is the intrinsic spatial curvature. We use natural units such that the speed of light  $c = 1$  and hence we have the Planck mass  $M_P = G_N^{-1/2} \simeq 10^{19}$  GeV. A cosmological constant,  $\Lambda$ , of the magnitude required to accelerate the Universe today (see Chap. 27, “Dark Energy” review) would have been completely negligible in the early Universe where the energy density  $\rho \gg M_P^2 \Lambda \sim 10^{-12}(\text{eV})^4$ . The standard early Universe cosmology, described in Sec. 22.1.5 in “Big Bang Cosmology” review, is thus dominated by non-relativistic matter ( $p_m = 0$ ) or radiation ( $p_r = \rho_r/3$  for an isotropic distribution). This leads to a decelerating expansion with  $\ddot{R} < 0$ .

The hypothesis of inflation [1,2] postulates a period of accelerated expansion,  $\ddot{R} > 0$ , in the very early Universe, preceding the standard radiation-dominated era, which offers a physical model for the origin of these initial conditions, as reviewed in [3,4,5,6,7]. Such a period of accelerated expansion (i) drives a curved RW spacetime (with spherical or hyperbolic spatial geometry) towards spatial flatness, and (ii) it also expands the causal horizon beyond the present Hubble length, so as to encompass all the scales relevant to describe the large-scale structure observed in our Universe today, via the following two mechanisms.

- (i) A spatially-flat universe with vanishing spatial curvature,  $k = 0$ , has the dimensionless density parameter  $\Omega_{\text{tot}} = 1$ , where we define (Eq. (22.13) in “Big Bang Cosmology” review; see Chap. 25, “Cosmological Parameters” review for more complete definitions)

$$\Omega_{\text{tot}} \equiv \frac{8\pi\rho_{\text{tot}}}{3M_P^2 H^2}, \quad (23.2)$$

## 2 23. Inflation

with  $\rho_{\text{tot}} \equiv \rho + \Lambda M_P^2/8\pi$ . If we re-write the Friedmann constraint (Eq. (23.1)) in terms of  $\Omega_{\text{tot}}$  we have

$$1 - \Omega_{\text{tot}} = -\frac{k}{\dot{R}^2}. \quad (23.3)$$

Observations require  $|1 - \Omega_{\text{tot},0}| < 0.005$  today [8], where the subscript 0 denotes the present-day value. Taking the time derivative of Eq. (23.3) we obtain

$$\frac{d}{dt}(1 - \Omega_{\text{tot}}) = -2\frac{\ddot{R}}{\dot{R}}(1 - \Omega_{\text{tot}}). \quad (23.4)$$

Thus in a decelerating expansion,  $\dot{R} > 0$  and  $\ddot{R} < 0$ , any small initial deviation from spatial flatness grows,  $(d/dt)|1 - \Omega_{\text{tot}}| > 0$ . A small value such as  $|1 - \Omega_{\text{tot},0}| < 0.005$  today requires an even smaller value at earlier times, e.g.,  $|1 - \Omega_{\text{tot}}| < 10^{-5}$  at the last scattering of the CMB, which appears unlikely, unless for some reason space is exactly flat. However, an extended period of accelerated expansion in the very early Universe, with  $\dot{R} > 0$  and  $\ddot{R} > 0$  and hence  $(d/dt)|1 - \Omega_{\text{tot}}| < 0$ , can drive  $\Omega_{\text{tot}}$  sufficiently close to unity, so that  $|1 - \Omega_{\text{tot},0}|$  remains unobservably small today, even after the radiation- and matter-dominated eras, for a wide range of initial values of  $\Omega_{\text{tot}}$ .

- (ii) The comoving distance (the present-day proper distance) traversed by light between cosmic time  $t_1$  and  $t_2$  in an expanding universe can be written, (see Eq. (22.31) in “Big Bang Cosmology” review), as

$$D_0(t_1, t_2) = R_0 \int_{t_1}^{t_2} \frac{dt}{R(t)} = R_0 \int_{\ln R_1}^{\ln R_2} \frac{d(\ln R)}{\dot{R}}. \quad (23.5)$$

In standard decelerated (radiation- or matter-dominated) cosmology the integrand,  $1/\dot{R}$ , decreases towards the past, and there is a finite comoving distance traversed by light (a particle horizon) since the Big Bang ( $R_1 \rightarrow 0$ ). For example, the comoving size of the particle horizon at the CMB last-scattering surface ( $R_2 = R_{\text{lss}}$ ) corresponds to  $D_0 \sim 100$  Mpc, or approximately  $1^\circ$  on the CMB sky today (see Sec. 22.2.4 in “Big Bang Cosmology” review).

However, during a period of inflation,  $1/\dot{R}$  increases towards the past, and hence the integral (Eq. (23.5)) diverges as  $R_1 \rightarrow 0$ , allowing an arbitrarily large causal horizon, dependent only upon the duration of the accelerated expansion. Assuming that the Universe inflates with a finite Hubble rate  $H_*$  at  $t_1 = t_*$ , ending with  $H_{\text{end}} < H_*$  at  $t_2 = t_{\text{end}}$ , we have

$$D_0(t_*, t_{\text{end}}) > \left(\frac{R_0}{R_{\text{end}}}\right) H_*^{-1} (e^{N_*} - 1), \quad (23.6)$$

where  $N_* \equiv \ln(R_{\text{end}}/R_*)$  describes the duration of inflation, measured in terms of the logarithmic expansion (or “e-folds”) from  $t_1 = t_*$  up to the end of inflation at  $t_2 = t_{\text{end}}$ , and  $R_0/R_{\text{end}}$  is the subsequent expansion from the end of inflation to the present day. If inflation occurs above the TeV scale, the comoving Hubble scale at the end of inflation,

$(R_0/R_{\text{end}})H_{\text{end}}^{-1}$ , is less than one astronomical unit ( $\sim 10^{11}$  m), and a causally-connected patch can encompass our entire observable Universe today, which has a size  $D_0 > 30$  Gpc, if there were more than 40 e-folds of inflation ( $N_* > 40$ ). If inflation occurs at the GUT scale ( $10^{15}$  GeV) then we require more than 60 e-folds.

Producing an accelerated expansion in general relativity requires an energy-momentum tensor with negative pressure,  $p < -\rho/3$  (see Eq. (22.9) in “Big Bang Cosmology” review and Chap. 27, “Dark Energy” review), quite different from the hot dense plasma of relativistic particles in the hot Big Bang. However a positive vacuum energy  $V > 0$  does exert a negative pressure,  $p_V = -\rho_V$ . The work done by the cosmological expansion must be negative in this case so that the local vacuum energy density remains constant in an expanding universe,  $\dot{\rho}_V = -3H(\rho_V + p_V) = 0$ . Therefore, a false vacuum state can drive an exponential expansion, corresponding to a de Sitter spacetime with a constant Hubble rate  $H^2 = 8\pi\rho_V/3M_P^2$  on spatially-flat hypersurfaces.

A constant vacuum energy  $V$ , equivalent to a cosmological constant  $\Lambda$  in the Friedmann equation, cannot provide a complete description of inflation in the early Universe, since inflation must necessarily have come to an end in order for the standard Big-Bang cosmology to follow. A phase transition to the present true vacuum is required to release the false vacuum energy into the energetic plasma of the hot Big Bang and produce the large total entropy of our observed Universe today. Thus we must necessarily study dynamical models of inflation, where the time-invariance of the false vacuum state is broken by a time-dependent field. A first-order phase transition would produce a very inhomogeneous Universe [9] unless a time-dependent scalar field leads to a rapidly changing percolation rate [10,11,12]. However, a second-order phase transition [13,14], controlled by a slowly-rolling scalar field, can lead to a smooth classical exit from the vacuum-dominated phase.

As a spectacular bonus, quantum fluctuations in that scalar field could provide a source of almost scale-invariant density fluctuations [15,16], as detected in the CMB (see section CosmicMicrowaveBackground), which are thought to be the origin of the structures seen in the Universe today.

Accelerated expansion and primordial perturbations can also be produced in some modified gravity theories (e.g., [1,17]) , which introduce additional non-minimally coupled degrees of freedom. Such inflation models can often be conveniently studied by transforming variables to an ‘Einstein frame’ in which Einstein’s equations apply with minimally coupled scalar fields [18,19,20].

In the following we will review scalar field cosmology in general relativity and the spectra of primordial fluctuations produced during inflation, before studying selected inflation models.

## 4 23. Inflation

### 23.2. Scalar Field Cosmology

The energy-momentum tensor for a canonical scalar field  $\phi$  with self-interaction potential  $V(\phi)$  is given in Eq. (22.51) in “Big Bang Cosmology” review. In a homogeneous background this corresponds to a perfect fluid with density

$$\rho = \frac{1}{2}\dot{\phi}^2 + V(\phi), \quad (23.7)$$

and isotropic pressure

$$p = \frac{1}{2}\dot{\phi}^2 - V(\phi), \quad (23.8)$$

while the 4-velocity is proportional to the gradient of the field,  $u^\mu \propto \nabla^\mu \phi$ .

A field with vanishing potential energy acts like a stiff fluid with  $p = \rho = \dot{\phi}^2/2$ , whereas if the time-dependence vanishes we have  $p = -\rho = -V$  and the scalar field is uniform in time and space. Thus a classical, potential-dominated scalar-field cosmology, with  $p \simeq -\rho$ , can naturally drive a quasi-de Sitter expansion; the slow time-evolution of the energy density weakly breaks the exact  $O(1,3)$  symmetry of four-dimensional de Sitter spacetime down to a Robertson-Walker (RW) spacetime, where the scalar field plays the role of the cosmic time coordinate.

In a scalar-field RW cosmology the Friedmann constraint equation (Eq. (23.1)) reduces to

$$H^2 = \frac{8\pi}{3M_P^2} \left( \frac{1}{2}\dot{\phi}^2 + V \right) - \frac{k}{R^2}, \quad (23.9)$$

while energy conservation (Eq. (22.10) in “Big Bang Cosmology” review) for a homogeneous scalar field reduces to the Klein-Gordon equation of motion (Eq. (22.53) in “Big Bang Cosmology” review)

$$\ddot{\phi} = -3H\dot{\phi} - V'(\phi). \quad (23.10)$$

The evolution of the scalar field is thus driven by the potential gradient  $V' = dV/d\phi$ , subject to damping by the Hubble expansion  $H\dot{\phi}$ .

If we define the Hubble slow-roll parameter

$$\epsilon_H \equiv -\frac{\dot{H}}{H^2}, \quad (23.11)$$

then we see that inflation ( $\ddot{R} > 0$  and hence  $\dot{H} > -H^2$ ) requires  $\epsilon_H < 1$ . In this case the spatial curvature decreases relative to the scalar field energy density as the Universe expands. Hence in the following we drop the spatial curvature and consider a spatially-flat RW cosmology, assuming that inflation has lasted sufficiently long that our observable universe is very close to spatially flatness. However, we note that bubble nucleation, leading to a first-order phase transition during inflation, can lead to homogeneous hypersurfaces with a hyperbolic (‘open’) geometry, effectively resetting the spatial curvature inside the bubble [21]. This is the basis of so-called open inflation

models [22,23,24], where inflation inside the bubble has a finite duration, leaving a finite negative spatial curvature.

In a scalar field-dominated cosmology (Eq. (23.11)) gives

$$\epsilon_H = \frac{3\dot{\phi}^2}{2V + \dot{\phi}^2}, \quad (23.12)$$

in which case we see that inflation requires a potential-dominated expansion,  $\dot{\phi}^2 < V$ .

### 23.2.1. *Slow-Roll Inflation* :

It is commonly assumed that the field acceleration term,  $\ddot{\phi}$ , in (Eq. (23.10)) can be neglected, in which case one can give an approximate solution for the inflationary attractor [25]. This slow-roll approximation reduces the second-order Klein-Gordon equation (Eq. (23.10)) to a first-order system, which is over-damped, with the potential gradient being approximately balanced against to the Hubble damping:

$$3H\dot{\phi} \simeq -V', \quad (23.13)$$

and at the same time that the Hubble expansion (Eq. (23.9)) is dominated by the potential energy

$$H^2 \simeq \frac{8\pi}{3M_P^2} V(\phi), \quad (23.14)$$

corresponding to  $\epsilon_H \ll 1$ .

A necessary condition for the validity of the slow-roll approximation is that the potential slow-roll parameters

$$\epsilon \equiv \frac{M_P^2}{16\pi} \left( \frac{V'}{V} \right)^2, \quad \eta \equiv \frac{M_P^2}{8\pi} \left( \frac{V''}{V} \right), \quad (23.15)$$

are small, i.e.,  $\epsilon \ll 1$  and  $|\eta| \ll 1$ , requiring the potential to be correspondingly flat. If we identify  $V''$  with the effective mass of the field, we see that the slow-roll approximation requires that the mass of the scalar field must be small compared with the Hubble scale. We note that the Hubble slow-roll parameter coincides with the potential slow-roll parameter,  $\epsilon_H \simeq \epsilon$ , to leading order in the slow-roll approximation.

The slow-roll approximation allows one to determine the Hubble expansion rate as a function of the scalar field value, and vice versa. In particular, we can express, in terms of the scalar field value during inflation, the total logarithmic expansion, or number of “e-folds”:

$$N_* \equiv \ln \left( \frac{R_{\text{end}}}{R_*} \right) = \int_{t_*}^{t_{\text{end}}} H dt \simeq - \int_{\phi_*}^{\phi_{\text{end}}} \sqrt{\frac{4\pi}{\epsilon}} \frac{d\phi}{M_P} \text{ for } V' > 0. \quad (23.16)$$

Given that the slow-roll parameters are approximately constant during slow-roll inflation,  $d\epsilon/dN \simeq 2\epsilon(\eta - 2\epsilon) = \mathcal{O}(\epsilon^2)$ , we have

$$N_* \simeq \frac{4}{\sqrt{\epsilon}} \frac{\Delta\phi}{M_P}. \quad (23.17)$$

Since we require  $N > 40$  to solve the flatness, horizon and entropy problems of the standard Big Bang cosmology, we require either very slow roll,  $\epsilon < 0.01$ , or a large change in the value of the scalar field relative to the Planck scale,  $\Delta\phi > M_P$ .

## 6 23. Inflation

### 23.2.2. Reheating :

Slow-roll inflation can lead to an exponentially large universe, close to spatial flatness and homogeneity, but the energy density is locked in the potential energy of the scalar field, and needs to be converted to particles and thermalised to recover a hot Big Bang cosmology at the end of inflation [26,27]. This process is usually referred to as reheating, although there was not necessarily any preceding thermal era. Reheating can occur when the scalar field evolves towards the minimum of its potential, converting the potential energy first to kinetic energy. This can occur either through the breakdown of the slow-roll condition in single-field models, or due to an instability triggered by the inflaton reaching a critical value, in multi-field models known as hybrid inflation models [28].

Close to a simple minimum, the scalar field potential can be described by a quadratic function,  $V = m^2\phi^2/2$ , where  $m$  is the mass of the field. We can obtain slow-roll inflation in such a potential at large field values,  $\phi \gg M_P$ . However, for  $\phi \ll M_P$  the field approaches an oscillatory solution:

$$\phi(t) \simeq \frac{M_P}{\sqrt{3\pi}} \frac{\sin(mt)}{mt}. \quad (23.18)$$

For  $|\phi| < M_P$  the Hubble rate drops below the inflaton mass,  $H < m$ , and the field oscillates many times over a Hubble time. Averaging over several oscillations,  $\Delta t \gg m^{-1}$ , we find  $\langle \dot{\phi}^2/2 \rangle_{\Delta t} \simeq \langle m^2\phi^2/2 \rangle_{\Delta t}$  and hence

$$\langle \rho \rangle_{\Delta t} \simeq \frac{M_P^2}{6\pi t^2}, \quad \langle p \rangle_{\Delta t} \simeq 0. \quad (23.19)$$

This coherent oscillating field corresponds to a condensate of non-relativistic massive inflaton particles, driving a matter-dominated era at the end of inflation, with scale factor  $R \propto t^{2/3}$ .

The inflaton condensate can lose energy through perturbative decays due to terms in the interaction Lagrangian, such as

$$\mathcal{L}_{\text{int}} \subset -\lambda_i \sigma \phi \chi_i^2 - \lambda_j \phi \bar{\psi}_j \psi_j \quad (23.20)$$

that couple the inflation to scalar fields  $\chi_i$  or fermions  $\psi_j$ , where  $\sigma$  has dimensions of mass and the  $\lambda_i$  are dimensionless couplings. When the mass of the inflaton is much larger than the decay products, the decay rate is given by [29]

$$\Gamma_i = \frac{\lambda_i^2 \sigma^2}{8\pi m}, \quad \Gamma_j = \frac{\lambda_j^2 m}{8\pi}. \quad (23.21)$$

These decay products must in turn thermalise with Standard Model particles before we recover conventional hot Big Bang cosmology. An upper limit on the reheating temperature after inflation is given by [27]

$$T_{rh} = 0.2 \left( \frac{100}{g_*} \right)^{1/4} \sqrt{M_P \Gamma_{\text{tot}}}, \quad (23.22)$$

where  $g_*$  is the effective number of degrees of freedom and  $\Gamma_{\text{tot}}$  is the total decay rate for the inflaton, which is required to be less than  $m$  for perturbative decay.

The baryon asymmetry of the Universe must be generated after the main release of entropy during inflation, which is an important constraint on possible models. Also, the fact that the inflaton mass is much larger than the mass scale of the Standard Model opens up the possibility that it may decay into massive stable or metastable particles that could be connected with dark matter, constraining possible models. For example, in the context of supergravity models the reheat temperature is constrained by the requirement that gravitinos are not overproduced, potentially destroying the successes of Big Bang nucleosynthesis. For a range of gravitino masses one must require  $T_{rh} < 10^9$  GeV [30,31].

The process of inflaton decay and reheating can be significantly altered by interactions leading to space-time dependences in the effective masses of the fields. In particular, parametric resonance can lead to explosive, non-perturbative decay of the inflaton in some cases, a process often referred to as preheating [32,26]. For example, an interaction term of the form

$$\mathcal{L}_{\text{int}} \subset -\lambda^2 \phi^2 \chi^2, \quad (23.23)$$

leads to a time-dependent effective mass for the  $\chi$  field as the inflaton  $\phi$  oscillates. This can lead to non-adiabatic particle production if the bare mass of the  $\chi$  field is small for large couplings or for rapid changes of the inflaton field. The process of preheating is highly model-dependent, but it highlights the possible role of non-thermal particle production after and even during inflation.

### 23.3. Primordial Perturbations from Inflation

Although inflation was originally discussed as a solution to the problem of initial conditions required for homogeneous and isotropic hot Big Bang cosmology, it was soon realised that inflation also offered a mechanism to generate the inhomogeneous initial conditions required for the formation of large-scale structure [15,16,17,33].

#### 23.3.1. Metric Perturbations :

In a homogeneous classical inflationary cosmology driven by a scalar field, the inflaton field is uniform on constant-time hypersurfaces,  $\phi = \phi_0(t)$ . However, quantum fluctuations inevitably break the spatial symmetry leading to an inhomogeneous field:

$$\phi(t, x^i) = \phi_0(t) + \delta\phi(t, x^i). \quad (23.24)$$

At the same time, one should consider inhomogeneous perturbations of the RW spacetime metric (see, e.g., [34,35,36]) :

$$ds^2 = (1 + 2A)dt^2 - 2RB_i dt dx^i - R^2 [(1 + 2C)\delta_{ij} + \partial_i \partial_j E + h_{ij}] dx^i dx^j, \quad (23.25)$$

where  $A$ ,  $B$ ,  $E$  and  $C$  are scalar perturbations while  $h_{ij}$  represents transverse and tracefree, tensor metric perturbations. Vector metric perturbations can be eliminated using Einstein constraint equations in a scalar field cosmology.

## 8 23. Inflation

The tensor perturbations remain invariant under a temporal gauge transformation  $t \rightarrow t + \delta t(t, x^i)$ , but both the scalar field and the scalar metric perturbations transform. For example, we have

$$\delta\phi \rightarrow \delta\phi - \dot{\phi}_0 \delta t, \quad C \rightarrow C - H \delta t. \quad (23.26)$$

However, there are gauge invariant combinations, such as [37]

$$Q = \delta\phi - \frac{\dot{\phi}_0}{H} C, \quad (23.27)$$

which describes the scalar field perturbations on spatially-flat hypersurfaces. This is simply related to the curvature perturbation on uniform-field hypersurfaces:

$$\mathcal{R} = C - \frac{H}{\dot{\phi}_0} \delta\phi = -\frac{H}{\dot{\phi}_0} Q, \quad (23.28)$$

which coincides in slow-roll inflation,  $\rho \simeq \rho(\phi)$ , with the curvature perturbation on uniform-density hypersurfaces [16]

$$\zeta = C - \frac{H}{\dot{\rho}_0} \delta\rho. \quad (23.29)$$

Thus scalar field and scalar metric perturbations are coupled by the evolution of the inflaton field.

### 23.3.2. Gravitational waves from inflation :

The tensor metric perturbation,  $h_{ij}$  in Eq. (Eq. (23.25)), is gauge-invariant and decoupled from the scalar perturbations at first order. This represents the free excitations of the spacetime, i.e., gravitational waves, which are the simplest metric perturbations to study at linear order.

Each tensor mode, with wavevector  $\vec{k}$ , has two linearly-independent transverse and trace-free polarisation states:

$$h_{ij}(\vec{k}) = h_{\vec{k}} q_{ij} + \bar{h}_{\vec{k}} \bar{q}_{ij}. \quad (23.30)$$

The linearised Einstein equations then yield the same evolution equation for the amplitude as that for a massless field in RW spacetime:

$$\ddot{h}_{\vec{k}} + 3H\dot{h}_{\vec{k}} + \frac{k^2}{R^2} h_{\vec{k}} = 0, \quad (23.31)$$

(and similarly for  $\bar{h}_{\vec{k}}$ ). This can be re-written in terms of the conformal time,  $\eta = \int dt/R$ , and the conformally rescaled field:

$$u_{\vec{k}} = \frac{M_P R h_{\vec{k}}}{\sqrt{32\pi}}. \quad (23.32)$$

This conformal field then obeys the wave equation for a canonical scalar field in Minkowski spacetime with a time-dependent mass:

$$u_{\vec{k}}'' + \left( k^2 - \frac{R''}{R} \right) u_{\vec{k}} = 0. \quad (23.33)$$

During slow-roll

$$\frac{R''}{R} \simeq (2 - \epsilon) R^2 H^2. \quad (23.34)$$

This makes it possible on sub-Hubble scales,  $k^2/R^2 \gg H^2$ , where the background expansion can be neglected, to quantise the linearised metric fluctuations,  $u_{\vec{k}} \rightarrow \hat{u}_{\vec{k}}$ .

Crucially, in an inflationary expansion, where  $\ddot{R} > 0$ , the comoving Hubble length  $H^{-1}/R = 1/\dot{R}$  decreases with time. Thus all modes start inside the Hubble horizon and it is possible to take the initial field fluctuations to be in a vacuum state at early times or on small scales:

$$\langle u_{\vec{k}_1} u_{\vec{k}_2} \rangle = \frac{i}{2} (2\pi)^3 \delta^{(3)}(\vec{k}_1 + \vec{k}_2). \quad (23.35)$$

In terms of the amplitude of the tensor metric perturbations, this corresponds to

$$\langle h_{\vec{k}_1} h_{\vec{k}_2} \rangle = \frac{1}{2} \frac{\mathcal{P}_T(k_1)}{4\pi k_1^3} (2\pi)^3 \delta^{(3)}(\vec{k}_1 + \vec{k}_2), \quad (23.36)$$

where the factor 1/2 appears due to the two polarisation states that contribute to the total tensor power spectrum:

$$\mathcal{P}_t(k) = \frac{64\pi}{M_P^2} \left( \frac{k}{2\pi R} \right)^2. \quad (23.37)$$

On super-Hubble scales,  $k^2/R^2 \ll H^2$ , we have the growing mode solution,  $u_{\vec{k}} \propto R$ , corresponding to  $h_{\vec{k}} \rightarrow \text{constant}$ , i.e., tensor modes are frozen-in on super-Hubble scales, both during and after inflation. Thus, connecting the initial vacuum fluctuations on sub-Hubble scales to the late-time power spectrum for tensor modes at Hubble exit during inflation,  $k = R_* H_*$ , we obtain

$$\mathcal{P}_t(k) \simeq \frac{64\pi}{M_P^2} \left( \frac{H_*}{2\pi} \right)^2. \quad (23.38)$$

In the de Sitter limit,  $\epsilon \rightarrow 0$ , the Hubble rate becomes time-independent and the tensor spectrum on super-Hubble scales becomes scale-invariant [38]. However slow-roll evolution leads to weak time dependence of  $H_*$  and thus a scale-dependent spectrum on large scales, with a spectral tilt

$$n_t \equiv \frac{d \ln \mathcal{P}_T}{d \ln k} \simeq -2\epsilon_*. \quad (23.39)$$

## 10 23. Inflation

### 23.3.3. Density Perturbations from Inflation :

The scalar field fluctuations on spatially-flat hypersurfaces are coupled to scalar metric perturbations at first order, but these can be eliminated using the Einstein constraint equations to yield an evolution equation

$$\ddot{Q}_{\vec{k}} + 3H\dot{Q}_{\vec{k}} + \left[ \frac{k^2}{R^2} + V'' - \frac{8\pi}{3M_P^2} \frac{d}{dt} \left( \frac{R^3 \dot{\phi}^2}{H} \right) \right] Q_{\vec{k}} = 0. \quad (23.40)$$

Terms proportional to  $M_P^{-2}$  represent the effect on the field fluctuations of gravity at first order. As can be seen, this vanishes in the limit of a constant background field, and hence is suppressed in the slow-roll limit, but it is of the same order as the effective mass,  $V'' = 3\eta H^2$ , so must be included if we wish to model deviations from exact de Sitter symmetry.

This wave equation can also be written in the canonical form for a free field in Minkowski spacetime if we define [37]

$$v_{\vec{k}} \equiv RQ_{\vec{k}}, \quad (23.41)$$

to yield

$$v_{\vec{k}}'' + \left( k^2 - \frac{z''}{z} \right) v_{\vec{k}} = 0, \quad (23.42)$$

where we define

$$z \equiv \frac{R\dot{\phi}}{H}, \quad \frac{z''}{z} \simeq (2 + 5\epsilon - 3\eta)R^2 H^2, \quad (23.43)$$

where the last approximate equality holds to leading order in the slow-roll approximation.

As previously done for gravitational waves, we quantise the linearised field fluctuations  $v_{\vec{k}} \rightarrow \hat{v}_{\vec{k}}$  on sub-Hubble scales,  $k^2/R^2 \gg H^2$ , where the background expansion can be neglected. Thus we impose

$$\langle v_{\vec{k}_1} v_{\vec{k}_2} \rangle = \frac{i}{2} (2\pi)^3 \delta^{(3)}(\vec{k}_1 + \vec{k}_2). \quad (23.44)$$

In terms of the field perturbations, this corresponds to

$$\langle Q_{\vec{k}_1} Q_{\vec{k}_2} \rangle = \frac{\mathcal{P}_Q(k_1)}{4\pi k_1^3} (2\pi)^3 \delta^{(3)}(\vec{k}_1 + \vec{k}_2), \quad (23.45)$$

where the power spectrum for vacuum field fluctuations on sub-Hubble scales,  $k^2/R^2 \gg H^2$ , is simply

$$\mathcal{P}_Q(k) = \left( \frac{k}{2\pi R} \right)^2, \quad (23.46)$$

yielding the classic result for the vacuum fluctuations for a massless field in de Sitter at Hubble exit,  $k = R_* H_*$ :

$$\mathcal{P}_Q(k) \simeq \left( \frac{H}{2\pi} \right)_*^2. \quad (23.47)$$

In practice there are slow-roll corrections due to the small but finite mass ( $\eta$ ) and field evolution ( $\epsilon$ ) [39].

Slow-roll corrections to the field fluctuations are small on sub-Hubble scales, but can become significant as the field and its perturbations evolve over time on super-Hubble scales. Thus it is helpful to work instead with the curvature perturbation,  $\zeta$  defined in equation (Eq. (23.29)), which remains constant on super-Hubble scales for adiabatic density perturbations both during and after inflation [16,40]. Thus we have an expression for the primordial curvature perturbation on super-Hubble scales produced by single-field inflation:

$$\mathcal{P}_\zeta(k) = \left[ \left( \frac{H}{\dot{\phi}} \right)^2 \mathcal{P}_Q(k) \right]_* \simeq \frac{4\pi}{M_P^2} \left[ \frac{1}{\epsilon} \left( \frac{H}{2\pi} \right)^2 \right]_* . \quad (23.48)$$

Comparing this with the primordial gravitational wave power spectrum (Eq. (23.38)) we obtain the tensor-to-scalar ratio for single-field slow-roll inflation

$$r \equiv \frac{\mathcal{P}_\zeta}{\mathcal{P}_t} \simeq 16\epsilon_* . \quad (23.49)$$

Note that the scalar amplitude is boosted by a factor  $1/\epsilon_*$  during slow-roll inflation, because small scalar field fluctuations can lead to relatively large curvature perturbations on hypersurfaces defined with respect to the density if the potential energy is only weakly dependent on the scalar field, as in slow-roll. Indeed, the de Sitter limit is singular, since the potential energy becomes independent of the scalar field at first order,  $\epsilon \rightarrow 0$ , and the curvature perturbation on uniform-density hypersurfaces becomes ill-defined.

We note that in single-field inflation the tensor-to-scalar ratio and the tensor tilt (Eq. (23.39)) at the same scale are both determined by the first slow-roll parameter at Hubble exit,  $\epsilon_*$ , giving rise to an important consistency test for single-field inflation:

$$n_t = -\frac{r}{8} . \quad (23.50)$$

This may be hard to verify if  $r$  is small, making any tensor tilt  $n_t$  difficult to measure. On the other hand, it does offer a way to rule out single-field slow-roll inflation if either  $r$  or  $n_t$  is large.

Given the relatively large scalar power spectrum, it has proved easier to measure the scalar tilt, conventionally defined as  $n_s - 1$ . Slow-roll corrections lead to slow time-dependence of both  $H_*$  and  $\epsilon_*$ , giving a weak scale-dependence of the scalar power spectrum:

$$n_s - 1 \equiv \frac{d \ln \mathcal{P}_\zeta}{d \ln k} \simeq -6\epsilon_* + 2\eta_* , \quad (23.51)$$

and a running of this tilt at second-order in slow-roll:

$$\frac{dn_s}{d \ln k} \simeq -8\epsilon_*(3\epsilon_* - 2\eta_*) - 2\xi_*^2 , \quad (23.52)$$

## 12 23. Inflation

where the running introduces a new slow-roll parameter at second-order:

$$\xi^2 = \frac{M_P^4}{64\pi^2} \frac{V'V'''}{V^2}. \quad (23.53)$$

Any relation between the tensor-to-scalar ratio and the scalar tilt must impose some model-dependent relation between the slow-roll parameters. For example, for power-law inflation or chaotic inflation driven by a massive field (see later) we have  $\eta \simeq \epsilon$  and hence

$$n_s - 1 \simeq -\frac{r}{8}. \quad (23.54)$$

Violating this condition would rule out these specific classes of single-field models.

### 23.3.4. Observational Bounds :

The observed scale-dependence of the power spectrum makes it necessary to specify the comoving scale,  $k$ , at which quantities are constrained and hence the Hubble-exit time,  $k = a_* H_*$ , when the corresponding theoretical quantities are calculated during inflation. This is usually expressed in terms of the number of e-folds from the end of inflation [41]:

$$N_*(k) \simeq 67 - \ln\left(\frac{k}{a_0 H_0}\right) + \frac{1}{4} \ln\left(\frac{V_*^2}{M_P^4 \rho_{\text{end}}}\right) + \frac{1}{12} \ln\left(\frac{\rho_{rh}}{\rho_{\text{end}}}\right) - \frac{1}{12} \ln(g_*), \quad (23.55)$$

where  $H_0^{-1}/a_0$  is the present comoving Hubble length. Different models of reheating and thus different reheat temperatures and densities,  $\rho_{rh}$  in Eq. (23.55), lead to a range of possible values for  $N_*$  corresponding to a fixed physical scale, and hence we have a range of observational predictions for a given inflation model, as seen in Fig. 23.1.

The Planck 2015 temperature and polarisation data (see Chap. 28, ‘‘Cosmic Microwave Background’’ review) are consistent with a smooth featureless power spectrum over a range of comoving wavenumbers,  $0.008 h^{-1} \text{ Mpc}^{-1} \leq k \leq 0.1 h \text{ Mpc}^{-1}$ . In the absence of running, the data measure the the spectral index

$$n_s = 0.968 \pm 0.006, \quad (23.56)$$

corresponding to a deviation from scale-invariance exceeding the  $5\sigma$  level. If running of the spectral tilt is included in the model, this is constrained to be

$$\frac{dn_s}{d \ln k} = -0.003 \pm 0.007. \quad (23.57)$$

A recent analysis of the BICEP2/Keck Array, Planck and other data places an upper bound on the tensor-to-scalar ratio [42]

$$r < 0.07 \quad (23.58)$$

at the 95% CL.

These observational bounds can be converted into bounds on the slow-roll parameters and hence the potential during slow-roll inflation. Setting higher-order slow-roll parameters (beyond second-order in horizon-flow parameters [43]) to zero the Planck collaboration obtain the following bounds [44]

$$\epsilon < 0.012, \quad (23.59)$$

$$\eta = -0.0080^{+0.0088}_{-0.0146}, \quad (23.60)$$

$$\xi^2 = 0.0070^{+0.0045}_{-0.0069}, \quad (23.61)$$

which can be used to constrain models, as discussed in the next Section.

Fig. 23.1, which is taken from [44], compares observational CMB constraints on the tilt,  $n_s$ , in the spectrum of scalar perturbations and the ratio,  $r$ , between the magnitudes of tensor and scalar perturbations. Important rôles are played by data from the Planck satellite, the BICEP2/Keck Array (BKP) and measurements of baryon acoustic oscillations (BAO). The reader is referred to [44] for technical details. These experimental constraints are compared with the predictions of some of the inflationary models discussed in this review. Generally speaking, models with a concave potential are favoured over those with a convex potential, and models with power-law inflation, as opposed to de Sitter-like (quasi-)exponential expansion, are now excluded.

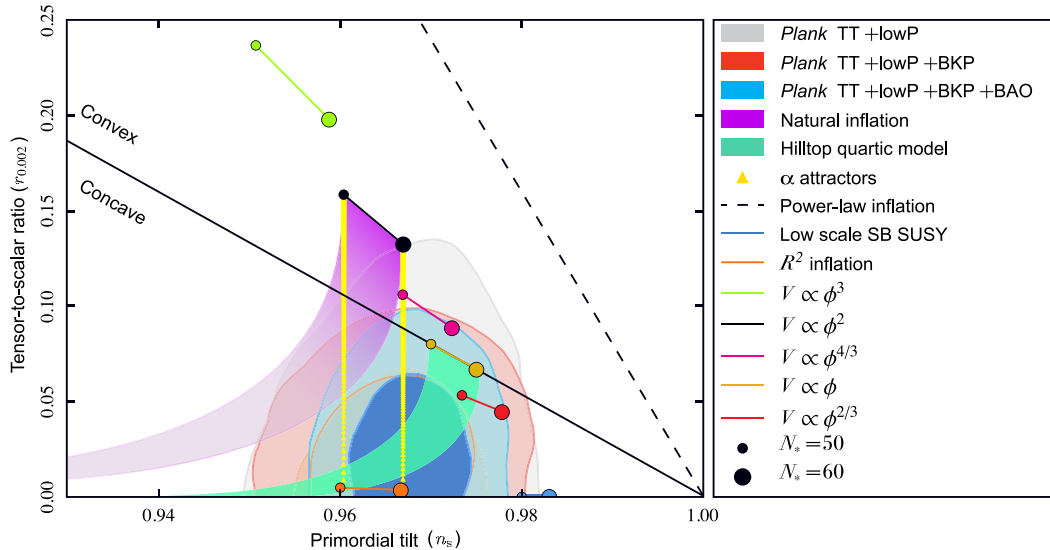


**Figure 23.1:** The marginalized joint 68 and 95% CL regions for the tilt in the scalar perturbation spectrum,  $n_s$ , and the relative magnitude of the tensor perturbations,  $r$ , obtained from the Planck 2015 data and their combinations with BICEP2/Keck Array and/or BAO data, confronted with the predictions of some of the inflationary models discussed in this review. This figure is taken from [44].

## 14 23. Inflation

### 23.4. Models

#### 23.4.1. Pioneering Models :

The paradigm of the inflationary Universe was proposed in [2], where it was pointed out that an early period of (near-)exponential expansion, in addition to resolving the horizon and flatness problems of conventional Big-Bang cosmology as discussed above (the possibility of a de Sitter phase in the early history of the Universe was also proposed in the non-minimal gravity model of [1], with the motivation of avoiding an initial singularity), would also dilute the prior abundance of any unseen heavy, (meta-)stable particles, as exemplified by monopoles in grand unified theories (GUTs; see Chap. 16, “Grand Unified Theories” review). The original proposal was that this inflationary expansion took place while the Universe was in a metastable state (a similar suggestion was made in [45,46], where in [45] it was also pointed out that such a mechanism could address the horizon problem) and was terminated by a first-order transition due to tunnelling through a potential barrier. However, it was recognized already in [2] that this ‘old inflation’ scenario would need modification if the transition to the post-inflationary universe were to be completed smoothly without generating unacceptable inhomogeneities.

This ‘graceful exit’ problem was addressed in the ‘new inflation’ model of [13] (see also [14] and footnote [39] of [2]), which studied models based on an SU(5) GUT with an effective potential of the Coleman-Weinberg type (i.e., dominated by radiative corrections), in which inflation could occur during the roll-down from the local maximum of the potential towards a global minimum. However, it was realized that the Universe would evolve to a different minimum from the Standard Model [47], and it was also recognized that density fluctuations would necessarily be too large [15], since they were related to the GUT coupling strength.

These early models of inflation assumed initial conditions enforced by thermal equilibrium in the early Universe. However, this assumption was questionable: indeed, it was not made in the model of [1], in which a higher-order gravitational curvature term was assumed to arise from quantum corrections, and the assumption of initial thermal equilibrium was jettisoned in the ‘chaotic’ inflationary model of [48]. These are the inspirations for much recent inflationary model building, so we now discuss them in more detail, before reviewing contemporary models.

In this section we will work in natural units where we set the reduced Planck mass to unity, i.e.,  $8\pi/M_P^2 = 1$ . All masses are thus relative to the reduced Planck scale.

#### 23.4.2. $R^2$ Inflation :

The first-order Einstein-Hilbert action,  $(1/2) \int d^4x \sqrt{-g} R$ , where  $R$  is the Ricci scalar curvature, is the minimal possible theory consistent with general coordinate invariance. However, it is possible that there might be non-minimal corrections to this action, and the unique second-order possibility is

$$S = \frac{1}{2} \int d^4x \sqrt{-g} \left( R + \frac{R^2}{6M^2} \right). \quad (23.62)$$

It was pointed out in [1] that an  $R^2$  term could be generated by quantum effects, and that (Eq. (23.62)) could lead to de Sitter-like expansion of the Universe. Scalar density perturbations in this model were calculated in [17]. Because the initial phase was (almost) de Sitter, these perturbations were (approximately) scale-invariant, with magnitude  $\propto M$ . It was pointed out in [17] that requiring the scalar density perturbations to lie in the range  $10^{-3}$  to  $10^{-5}$ , consistent with upper limits at that time, would require  $M \sim 10^{-3}$  to  $10^{-5}$  in Planck units, and it was further suggested in that these perturbations could lead to the observed large-scale structure of the Universe, including the formation of galaxies.

Although the action (Eq. (23.62)) does not contain an explicit scalar field, [17] reduced the calculation of density perturbations to that of fluctuations in the scalar curvature  $R$ , which could be identified (up to a factor) with a scalar field of mass  $M$ . The formal equivalence of  $R^2$  gravity (Eq. (23.62)) to a theory of gravity with a massive scalar  $\phi$  had been shown in [18], see also [19]. The effective scalar potential for what we would nowadays call the ‘inflaton’ [49] takes the form

$$S = \frac{1}{2} \int d^4x \sqrt{-g} \left[ R + (\partial_\mu \phi)^2 - \frac{3}{2} M^2 (1 - e^{-\sqrt{2/3} \phi})^2 \right] \quad (23.63)$$

when the action is written in the Einstein frame, and the potential is shown as the solid black line in Fig. 23.2. Using (Eq. (23.48)), one finds that the amplitude of the scalar density perturbations in this model is given by

$$\Delta_{\mathcal{R}} = \frac{3M^2}{8\pi^2} \sinh^4 \left( \frac{\phi}{\sqrt{6}} \right), \quad (23.64)$$

The measured magnitude of the density fluctuations in the CMB requires  $M \simeq 1.3 \times 10^{-5}$  in Planck units (assuming  $N_* \simeq 55$ ), so one of the open questions in this model is why  $M$  is so small. Obtaining  $N_* \simeq 55$  also requires an initial value of  $\phi \simeq 5.5$ , i.e., a super-Planckian initial condition, and another issue for this and many other models is how the form of the effective potential is protected and remains valid at such large field values. Using Eq. (23.51) one finds that  $n_s \simeq 0.965$  for  $N_* \simeq 55$  and using (Eq. (23.49)) one finds that  $r \simeq 0.0035$ . These predictions are consistent with the present data from Planck and other experiments, as seen in Fig. 23.1.

### 23.4.3. Chaotic Models with Power-Law Potentials :

As has already been mentioned, a key innovation in inflationary model-building was the suggestion to abandon the questionable assumption of a thermal initial state, and consider ‘chaotic’ initial conditions with very general forms of potential [48]. (Indeed, the  $R^2$  model discussed above can be regarded as a prototype of this approach.) The chaotic approach was first proposed in the context of a simple power-law potential of the form  $\mu^{4-\alpha} \phi^\alpha$ , and the specific example of  $\lambda \phi^4$  was studied in [48]. Such models make the following predictions for the slow-roll parameters  $\epsilon$  and  $\eta$ :

$$\epsilon = \frac{1}{2} \left( \frac{\alpha}{\phi} \right)^2, \quad \eta = \frac{\alpha(\alpha - 1)}{\phi^2}, \quad (23.65)$$

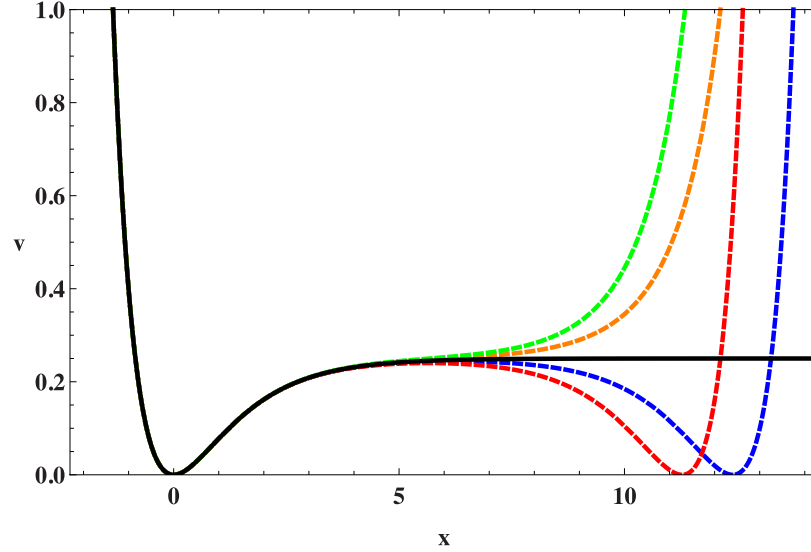


**Figure 23.2:** The inflationary potential  $V$  in the  $R^2$  model (solid black line) compared with its form in various no-scale models discussed in detail in [50] (dashed coloured lines).

leading to the predictions

$$r \approx \frac{4\alpha}{N_*}, \quad n_s - 1 \approx -\frac{\alpha + 2}{2N_*}, \quad (23.66)$$

which are shown in Fig. 23.1 for some illustrative values of  $\alpha$ . We note that the prediction of the original  $\phi^4$  model lies out of the frame, with values of  $r$  that are too large and values of  $n_s$  that are too small. The  $\phi^3$  model has similar problems, and would in any case require modification in order to have a well-defined minimum. The simplest possibility is  $\phi^2$ , but this is now also disfavoured by the data, at the 95% CL if only the Planck data are considered, and more strongly if other data are included, as seen in Fig. 23.1. (For non-minimal models of quadratic inflation that avoid this problem, see, e.g., [51].)

Indeed, as can be seen in Fig. 23.1, all models with a convex potential (i.e., one curving upwards) are disfavoured compared to models with a concave potential. Thus, a model with a  $\phi^{2/3}$  potential may just be compatible with the data at the 68% CL, whereas linear and  $\phi^{4/3}$  potentials are allowed only at about the 95% CL.

#### 23.4.4. *Hilltop Models* :

This preference for a concave potential motivates interest in ‘hilltop’ models [52], whose starting-point is a potential of the form

$$V(\phi) = \Lambda^4 \left[ 1 - \left( \frac{\phi}{\mu} \right)^p + \dots \right], \quad (23.67)$$

where the ... represent extra terms that yield a positive semi-definite potential. To first order in the slow-roll parameters, when  $x \equiv \phi/\mu$  is small, one has

$$n_s \simeq 1 - p(p-1)\mu^{-2} \frac{x^{p-2}}{(1-x^p)} - \frac{3}{8}r, \quad r \simeq 8p^2\mu^{-2} \frac{x^{2p-2}}{(1-x^p)^2}. \quad (23.68)$$

As seen in Fig. 23.1, a hilltop model with  $p = 4$  can be compatible with the Planck and other measurements, if  $\mu \gg M_P$ .

**23.4.5. D-Brane Inflation :**

Many scenarios for inflation involving extra dimensions have been proposed, e.g., the possibility that observable physics resides on a three-dimensional brane, and that there is an inflationary potential that depends on the distance between our brane and an antibrane, with a potential of the form [53]

$$V(\phi) = \Lambda^4 \left[ 1 - \left( \frac{\mu}{\phi} \right)^p + \dots \right]. \quad (23.69)$$

In this scenario the effective potential vanishes in the limit  $\phi \rightarrow \infty$ , corresponding to complete separation between our brane and the antibrane. The predictions for  $n_s$  and  $r$  in this model can be obtained from (Eq. (23.68)) by exchanging  $p \leftrightarrow -p$ , and are also consistent with the Planck and other data.

**23.4.6. Natural Inflation :**

Also seen in Fig. 23.1 are the predictions of ‘natural inflation’ [54], in which one postulates a non-perturbative shift symmetry that suppresses quantum corrections, so that a hierarchically small scale of inflation,  $H \ll M_P$ , is technically natural. In the simplest models, there is a periodic potential of the form

$$V(\phi) = \Lambda^4 \left[ 1 + \cos \left( \frac{\phi}{f} \right) \right], \quad (23.70)$$

where  $f$  is a dimensional parameter reminiscent of an axion decay constant (see the next subsection) [55], which must have a value  $> M_P$ . Natural inflation can yield predictions similar to quadratic inflation (which are no longer favoured, as already discussed), but can also yield an effective convex potential. Thus, it may lead to values of  $r$  that are acceptably small, but for values of  $n_s$  that are in tension with the data, as seen in Fig. 23.1.

## 18 23. Inflation

### 23.4.7. Axion Monodromy Models :

The effective potentials in stringy models [56,57] motivated by axion monodromy may be of the form

$$V(\phi) = \mu^{4-\alpha}\phi^\alpha + \Lambda^4 e^{-C\left(\frac{\phi}{\phi_0}\right)^{p_\Lambda}} \cos\left[\gamma + \frac{\phi}{f}\left(\frac{\phi}{\phi_0}\right)^{p_f+1}\right], \quad (23.71)$$

where  $\mu, \Lambda, f$  and  $\phi_0$  are parameters with the dimension of mass, and  $C, p, p_\Lambda, p_f$  and  $\gamma$  are dimensionless constants, generalizing the potential ([54]) in the simplest models of natural inflation. The oscillations in (Eq. (23.71)) are associated with the axion field, and powers  $p_\Lambda, p_f \neq 0$  may arise from  $\phi$ -dependent evolutions of string moduli. Since the exponential prefactor in (Eq. (23.71)) is due to non-perturbative effects that may be strongly suppressed, the oscillations may be unobservably small. Specific string models having  $\phi^\alpha$  with  $\alpha = 4/3, 1$  or  $2/3$  have been constructed in [56,57], providing some motivation for the low-power models mentioned above.

As seen in Fig. 23.1, the simplest axion monodromy models with these values of the power  $\alpha$  are compatible with all the available data at the 95% CL, though not at the 68% CL. The Planck Collaboration has also searched for characteristic effects associated with the second term in (Eq. (23.71)), such as a possible drift in the modulation amplitude (setting  $p_\Lambda = C = 0$ ), and a possible drifting frequency generated by  $p_f \neq 0$ , without finding any compelling evidence [44].

### 23.4.8. Higgs Inflation :

Since the energy scale during inflation is commonly expected to lie between the Planck and TeV scales, it may serve as a useful bridge with contacts both to string theory or some other quantum theory of gravity, on the one side, and particle physics on the other side. However, as the above discussion shows, much of the activity in building models of inflation has been largely independent of specific connections with these subjects, though some examples of string-motivated models of inflation were mentioned above.

The most economical scenario for inflation might be to use as inflaton the only established scalar field, namely the Higgs field (see Chap. 11, ‘‘Status of Higgs boson physics’’ review). A specific model assuming a non-minimal coupling of the Higgs field  $h$  to gravity was constructed in [58]. Its starting-point is the action

$$S = \int d^4x \sqrt{-g} \left[ \frac{M^2 + \xi h^2}{2} R + \frac{1}{2} \partial_\mu h \partial^\mu h - \frac{\lambda}{4} (h^2 - v^2)^2 \right], \quad (23.72)$$

where  $v$  is the Higgs vacuum expectation value. The model requires  $\xi \gg 1$ , in which case it can be rewritten in the Einstein frame as

$$S = \int d^4x \sqrt{-g} \left[ \frac{1}{2} R + \frac{1}{2} \partial_\mu \chi \partial^\mu \chi - U(\chi) \right], \quad (23.73)$$

where the effective potential for the canonically-normalized inflaton field  $\chi$  has the form

$$U(\chi) = \frac{\lambda}{4\xi^2} \left[ 1 + \exp\left(-\frac{2\chi}{\sqrt{6}M_P}\right) \right]^{-2}, \quad (23.74)$$

which is similar to the effective potential of the  $R^2$  model at large field values. As such, the model inflates successfully if  $\xi \simeq 5 \times 10^4 m_h/(\sqrt{2}v)$ , with predictions for  $n_s$  and  $r$  that are indistinguishable from the predictions of the  $R^2$  model shown in Fig. 23.1.

This model is very appealing, but must confront several issues. One is to understand the value of  $\xi$ , and another is the possibility of unitarity violation. However, a more fundamental issue is whether the effective quartic Higgs coupling is positive at the scale of the Higgs field during inflation. Extrapolations of the effective potential in the Standard Model using the measured values of the masses of the Higgs boson and the top quark indicate that probably  $\lambda < 0$  at this scale [59], though there are still significant uncertainties associated with the appropriate input value of the top mass and the extrapolation to high renormalization scales.

#### 23.4.9. *Supersymmetric Models of Inflation :*

Supersymmetry [60] is widely considered to be a well-motivated possible extension of the Standard Model that might become apparent at the TeV scale. It is therefore natural to consider supersymmetric models of inflation. These were originally proposed because of the problems of the the new inflationary theory [13,14] based on the one-loop (Coleman-Weinberg) potential for breaking SU(5). Several of these problems are related to the magnitude of the effective potential parameters: in any model of inflation based on an elementary scalar field, some parameter in the effective potential must be small in natural units, e.g., the quartic coupling  $\lambda$  in a chaotic model with a quartic potential, or the mass parameter  $\mu$  in a model of chaotic quadratic inflation. These parameters are renormalized multiplicatively in a supersymmetric theory, so that the quantum corrections to small values would be under control. Hence it was suggested that inflation cries out for supersymmetry [61], though non-supersymmetric resolutions of the problems of Coleman-Weinberg inflation are also possible: see, e.g., Ref. [62].

In the Standard Model there is only one scalar field that could be a candidate for the inflaton, namely the Higgs field discussed above, but even the minimal supersymmetric extension of the Standard Model (MSSM) contains many scalar fields. However, none of these is a promising candidate for the inflaton. The minimal extension of the MSSM that may contain a suitable candidate is the supersymmetric version of the minimal seesaw model of neutrino masses, which contains the three supersymmetric partners of the heavy singlet (right-handed) neutrinos. One of these singlet sneutrinos  $\tilde{\nu}$  could be the inflaton [63]: it would have a quadratic potential, the mass coefficient required would be  $\sim 10^{13}$  GeV, very much in the expected ball-park for singlet (right-handed) neutrino masses, and sneutrino inflaton decays also could give rise to the cosmological baryon asymmetry via leptogenesis. However, as seen in Fig. 23.1 and already discussed, a purely quadratic inflationary potential is no longer favoured by the data. This difficulty could in principle be resolved in models with multiple sneutrinos [64], or by postulating a trilinear sneutrino coupling and hence a superpotential of Wess-Zumino type [65], which can yield successful inflation with predictions intermediate between those of natural inflation and hilltop inflation in Fig. 23.1.

Finally, we note that it is also possible to obtain inflation via supersymmetry breaking, as in the model [66] whose predictions are illustrated in Fig. 23.1.

## 20 23. Inflation

### 23.4.10. Supergravity Models :

Any model of early-Universe cosmology, and specifically inflation, must necessarily incorporate gravity. In the context of supersymmetry this requires an embedding in some supergravity theory [67,68]. An  $\mathcal{N} = 1$  supergravity theory is specified by three functions: a Hermitian function of the matter scalar fields  $\phi^i$ , called the Kähler potential  $K$ , that describes its geometry, a holomorphic function of the superfields, called the superpotential  $W$ , which describes their interactions, and another holomorphic function  $f_{\alpha\beta}$ , which describes their couplings to gauge fields  $V_\alpha$  [69].

The simplest possibility is that the Kähler metric is flat:

$$K = \phi^i \phi_i^*, \quad (23.75)$$

where the sum is over all scalar fields in the theory, and the simplest inflationary model in minimal supergravity had the superpotential [70]

$$W = m^2(1 - \phi)^2, \quad (23.76)$$

Where  $\phi$  is the inflaton. However, this model predicts a tilted scalar perturbation spectrum,  $n_s = 0.933$ , which is now in serious disagreement with the data from Planck and other experiments shown in Fig. 23.1.

Moreover, there is a general problem that arises in any supergravity theory coupled to matter, namely that, since its effective scalar potential contains a factor of  $e^K$ , scalars typically receive squared masses  $\propto H^2 \sim V$ , where  $H$  is the Hubble parameter [71], an issue called the ‘ $\eta$  problem’. The theory given by (Eq. (23.76)) avoids this  $\eta$  problem, but a generic supergravity inflationary model encounters this problem of a large inflaton mass. Moreover, there are additional challenges for supergravity inflation associated with the spontaneous breaking of local supersymmetry [72,73,74].

Various approaches to the  $\eta$  problem in supergravity have been proposed, including the possibility of a shift symmetry [75], and one possibility that has attracted renewed attention recently is no-scale supergravity [76,77]. This is a form of supergravity with a Kähler potential that can be written in the form [78]

$$K = -3 \ln \left( T + T^* - \frac{\sum_i |\phi^i|^2}{3} \right), \quad (23.77)$$

which has the special property that it naturally has a flat potential, at the classical level and before specifying a non-trivial superpotential. As such, no-scale supergravity is well-suited for constructing models of inflation. Adding to its attraction is the feature that compactifications of string theory to supersymmetric four-dimensional models yield effective supergravity theories of the no-scale type [79]. There are many examples of superpotentials that yield effective inflationary potentials for either the  $T$  field (which is akin to a modulus field in some string compactification) or a  $\phi$  field (generically representing matter) that are of the same form as the effective potential of the  $R^2$  model (Eq. (23.63)) when the magnitude of the inflaton field  $\gg 1$  in Planck units, as required to obtain sufficiently many e-folds of inflation,  $N_*$  [80,81]. This framework also offers the possibility of using a suitable superpotential to construct models with effective potentials that are similar, but not identical, to the  $R^2$  model, as shown by the dashed coloured lines in Fig. 23.2.

### 23.4.11. Other Exponential Potential Models :

This framework also offers the possibility [80] of constructing models in which the asymptotic constant value of the potential at large inflaton field values is approached via a different exponentially-suppressed term:

$$V(\phi) = A \left[ 1 - \delta e^{-B\phi} + \mathcal{O}(e^{-2B\phi}) \right], \quad (23.78)$$

where the magnitude of the scalar density perturbations fixes  $A$ , but  $\delta$  and  $B$  are regarded as free parameters. In the case of  $R^2$  inflation  $\delta = 2$  and  $B = \sqrt{2/3}$ . In a model such as (Eq. (23.78)), one finds at leading order in the small quantity  $e^{-B\phi}$  that

$$\begin{aligned} n_s &= 1 - 2B^2\delta e^{-B\phi}, \\ r &= 8B^2\delta^2 e^{-2B\phi}, \\ N_* &= \frac{1}{B^2\delta} e^{+B\phi}. \end{aligned} \quad (23.79)$$

yielding the relations

$$n_s = 1 - \frac{2}{N_*}, r = \frac{8}{B^2 N_*^2}. \quad (23.80)$$

This model leads to the class of predictions labelled by ‘ $\alpha$  attractors’ [82] in Fig. 23.1. There are generalizations of the simplest no-scale model (Eq. (23.77)) with prefactors before the  $\ln(\dots)$  that are 1 or 2, leading to larger values of  $B = \sqrt{2}$  or 1, respectively, and hence smaller values of  $r$  than in the  $R^2$  model.

## 23.5. Model Comparison

Given a particular inflationary model, one can obtain constraints on the model parameters, informed by the likelihood, corresponding to the probability of the data given a particular choice of parameters (see Chap. 39, “Statistics” review). In the light of the detailed constraints on the statistical distribution of primordial perturbations now inferred from high-precision observations of the cosmic microwave background, it is also possible to make quantitative comparison of the statistical evidence for or against different inflationary models. This can be done either by comparing the logarithm of the maximum likelihood that can be obtained for the data using each model, i.e., the minimum  $\chi^2$  (with some correction for the number of free parameters in each model), or by a Bayesian model comparison [83] (see also Sec. 39.3.3 in “Statistics” review).

In such a Bayesian model comparison one computes [7] the evidence,  $\mathcal{E}(\mathcal{D}|\mathcal{M}_A)$  for a model,  $\mathcal{M}_A$ , given the data  $\mathcal{D}$ . This corresponds to the likelihood,  $\mathcal{L}(\theta_{Aj}) = p(\mathcal{D}|\theta_{Aj}, \mathcal{M}_A)$ , integrated over the assumed prior distribution,  $\pi(\theta_{Aj}|\mathcal{M}_A)$ , for all the model parameters  $\theta_{Aj}$ :

$$\mathcal{E}(\mathcal{D}|\mathcal{M}_A) = \int \mathcal{L}(\theta_{Aj})\pi(\theta_{Aj}|\mathcal{M}_A)d\theta_{Aj}. \quad (23.81)$$

**Table 23.1:** Observational evidence for and against selected inflation models:  $\Delta\chi^2$  is determined relative to a baseline  $\Lambda$ CDM model, and the Bayes factors are calculated relative to Starobinsky  $R^2$  inflation. Results from Planck 2015 analysis [44].

Model	$\Delta\chi^2$	$\ln B_{A,\text{ref}}$
$R^2$ inflation	+0.8	0
Power-law potential $\phi^{2/3}$	+6.5	-2.4
Power-law potential $\phi^2$	+8.6	-4.7
Power-law potential $\phi^4$	+43.3	-23.3
Natural inflation	+7.2	-2.4
SUSY $\alpha$ -attractor	+0.7	-1.8

The posterior probability of the model given the data follows from Bayes’ theorem

$$p(\mathcal{M}_A|\mathcal{D}) = \frac{\mathcal{E}(\mathcal{D}|\mathcal{M}_A)\pi(\mathcal{M}_A)}{p(\mathcal{D})}, \quad (23.82)$$

where the prior probability of the model is given by  $\pi(\mathcal{M}_A)$ . Assuming that all models are equally likely a priori,  $\pi(\mathcal{M}_A) = \pi(\mathcal{M}_B)$ , the relative probability of model  $A$  relative to a reference model, in the light of the data, is thus given by the Bayes factor

$$B_{A,\text{ref}} = \frac{\mathcal{E}(\mathcal{D}|\mathcal{M}_A)}{\mathcal{E}(\mathcal{D}|\mathcal{M}_{\text{ref}})}. \quad (23.83)$$

Computation of the multi-dimensional integral (Eq. (23.81)) is a challenging numerical task. Even using an efficient sampling algorithm requires hundreds of thousands of likelihood computations for each model, though slow-roll approximations can be used to calculate rapidly the primordial power spectrum using the APSIC numerical library [7] for a large number of single-field, slow-roll inflation models.

The change in  $\chi^2$  for selected slow-roll models relative to a baseline  $\Lambda$ CDM model is given in Table 1 (taken from [44]). All the inflation models require some amplitude of tensors and so have an increased  $\chi^2$  with respect to the baseline  $\Lambda$ CDM model with a scalar tilt but no tensors. Table Table 23.1 also shows the Bayesian evidence for ( $\ln B_{A,\text{ref}} > 0$ ) or against ( $\ln B_{A,\text{ref}} < 0$ ) a selection of inflation models using the Planck analysis priors [44]. The Starobinsky  $R^2$  inflationary model may be chosen as a reference [44] that provides a good fit to current data. Higgs inflation [58] is indistinguishable using current data, making the model comparison “inconclusive” on the Jeffery’s scale ( $|\ln B_{A,\text{ref}}| < 1$ ). (Recall, though, that this model is disfavoured by the measured values of the Higgs and top quark masses [59].) On the other hand, there is now moderate evidence ( $|\ln B_{A,\text{ref}}| > 2.5$ ) against large-field models such as chaotic inflation with a quadratic potential and strong evidence ( $|\ln B_{A,\text{ref}}| > 5$ ) against chaotic inflation with a quartic potential. Indeed, over 30% of the slow-roll inflation models considered in Ref. [7] are strongly disfavoured by the Planck data.

The Bayes factors for a wide selection of slow-roll inflationary models are displayed in Fig. 23.3, which is adapted from Fig. 3 in [84], where more complete descriptions of the models and the calculations of the Bayes factors are given. Models discussed in this review are highlighted in yellow, and numbered as follows: (1)  $R^2$  inflation (Sec. 23.4) and models with similar predictions, such as Higgs inflation (Sec. 23.4) and no-scale supergravity inflation (Sec. 23.4); chaotic inflation models (2) with a  $\phi^2$  potential; (3) with a  $\phi^4$  potential; (4) with a  $\phi^{2/3}$  potential, and (5) with a  $\phi^p$  potential marginalising over  $p \in [0.2, 6]$  (Sec. 23.4); hilltop inflation models (6) with  $p = 2$ ; (7) with  $p = 4$  and (8) marginalising over  $p$  (Secinflation:models:hilltop); (9) brane inflation (Secinflation:models:brane); (10) natural inflation (Sec. 23.4); (11) exponential potential models such as  $\alpha$ -attractors (Sec. 23.4). As seen in Fig. 23.3 and discussed in the next Section, constraints on reheating are starting to provide additional information about models of inflation.

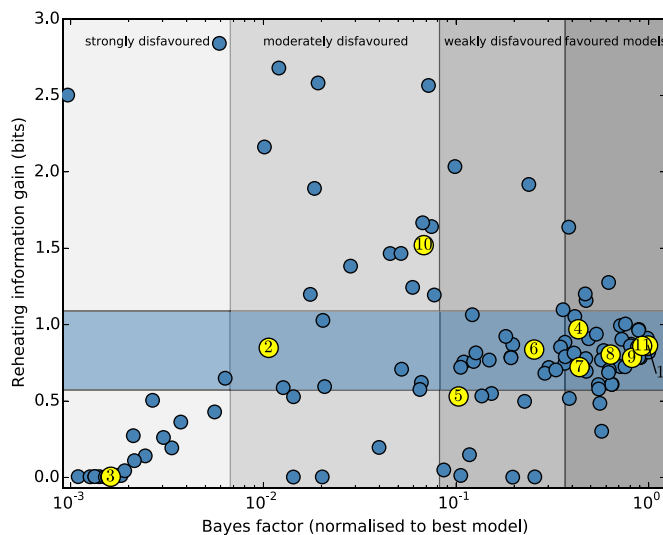


**Figure 23.3:** The Bayes factors calculated in [84] for a large sample of inflationary models. Those highlighted in yellow are featured in this review, according to the numbers listed in the text.

## 23.6. Constraints on Reheating

One connection between inflation and particle physics is provided by inflaton decay, whose products are expected to have thermalized subsequently. As seen in (Eq. (23.55)), the number of e-folds required during inflation depends on details of this reheating process, including the matter density upon reheating, denoted by  $\rho_{\text{th}}$ , which depends in turn on the inflaton decay rate  $\Gamma_\phi$ . We see in Fig. 23.1 that, within any specific inflationary model, both  $n_s$  and particularly  $r$  are sensitive to the value of  $N_*$ . In particular, the one- $\sigma$  uncertainty in the experimental measurement of  $n_s$  is comparable

## 24 23. Inflation

to the variation in many model predictions for  $N_* \in [50, 60]$ . This implies that the data start to constrain scenarios for inflaton decay in many models. For example, it is clear from Fig. 23.1 that  $N_* = 60$  would be preferred over  $N_* = 50$  in a chaotic inflationary model with a quadratic potential.

As a specific example, let us consider  $R^2$  models and related models such as Higgs and no-scale inflation models that predict small values of  $r$  [85]. As seen in Fig. 23.1, within these models the combination of Planck, BICEP2/Keck Array and BAO data would require a limited range of  $n_s$ , corresponding to a limited range of  $N_*$ , as seen by comparing the left and right vertical axes in Fig. 23.4:

$$N_* \gtrsim 52 \quad (68\% \text{ CL}), \quad N_* \gtrsim 44 \quad (95\% \text{ CL}). \quad (23.84)$$

Within any specific model for inflaton decay, these bounds can be translated into constraints on the effective decay coupling. For example, if one postulates a two-body inflaton decay coupling  $y$ , the bounds (Eq. (23.84)) can be translated into bounds on  $y$ . This is illustrated in Fig. 23.4, where any value of  $N_*$  (on the left vertical axis), projected onto the diagonal line representing the correlation predicted in  $R^2$ -like models, corresponds to a specific value of the inflaton decay rate  $\Gamma_\phi/m$  (lower horizontal axis) and hence  $y$  (upper horizontal axis):

$$y \gtrsim 10^{-5} \quad (68\% \text{ CL}), \quad y \gtrsim 10^{-15} \quad (95\% \text{ CL}). \quad (23.85)$$

These bounds are not very constraining – although the 68% CL lower bound on  $y$  is already comparable with the electron Yukawa coupling – but can be expected to improve significantly in the coming years and thereby provide significant information on the connections between inflation and particle physics.

### 23.7. Beyond Single-Field Slow-Roll Inflation

There are numerous possible scenarios beyond the simplest single-field models of slow-roll inflation. These include theories in which non-canonical fields are considered, such as k-inflation [86] or DBI inflation [87], and multiple-field models, such as the curvaton scenario [88]. As well as altering the single-field predictions for the primordial curvature power spectrum (Eq. (23.48)) and the tensor-scalar ratio (Eq. (23.49)), they may introduce new quantities that vanish in single-field slow-roll models, such as isocurvature matter perturbations, corresponding to entropy fluctuations in the photon-to-matter ratio, at first order:

$$S_m = \frac{\delta n_m}{n_m} - \frac{\delta n_\gamma}{n_\gamma} = \frac{\delta \rho_m}{\rho_m} - \frac{3}{4} \frac{\delta \rho_\gamma}{\rho_\gamma}. \quad (23.86)$$

Another possibility is non-Gaussianity in the distribution of the primordial curvature perturbation (see Chap. 28, “Cosmic Microwave Background” review), encoded in higher-order correlators such as the primordial bispectrum [89]

$$\langle \zeta(\mathbf{k})\zeta(\mathbf{k}')\zeta(\mathbf{k}'') \rangle \equiv (2\pi)^3 \delta(\mathbf{k} + \mathbf{k}' + \mathbf{k}'') B_\zeta(k, k', k''), \quad (23.87)$$

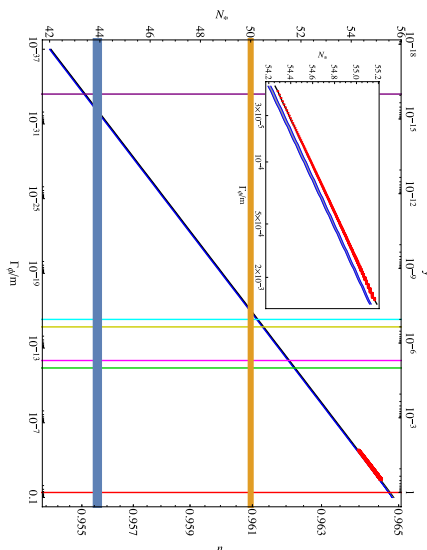


**Figure 23.4:** The values of  $N_*$  (left axis) and  $n_s$  (right axis) in  $R^2$  inflation and related models for a wide range of decay rates,  $\Gamma_\phi/m$ , (bottom axis) and corresponding two-body couplings,  $y$  (top axis). The diagonal red line segment shows full numerical results over a restricted range of  $\Gamma_\phi/m$  (which are shown in more detail in the insert), while the diagonal blue strip represents an analytical approximation described in [85]. The difference between these results is indistinguishable in the main plot, but is visible in the insert. The horizontal yellow and blue lines show the 68 and 95% CL lower limits from the Planck 2015 data [44], and the vertical coloured lines correspond to specific models of inflaton decay. Figure taken from [85].

which is often expressed in terms of a dimensionless non-linearity parameter  $f_{\text{NL}} \propto B_\zeta(k, k', k'')/P_\zeta(k)P_\zeta(k')$ . The three-point function (Eq. (23.87)) can be thought of as defined on a triangle whose sides are  $\mathbf{k}, \mathbf{k}', \mathbf{k}''$ , of which only two are independent, since they sum to zero. Further assuming statistical isotropy ensures that the bispectrum depends only on the magnitudes of the three vectors,  $k, k'$  and  $k''$ . The search for  $f_{\text{NL}}$  and other non-Gaussian effects was a prime objective of the Planck data analysis [90].

### 23.7.1. *Effective Field Theory of Inflation* :

Since slow-roll inflation is a phase of accelerated expansion with an almost constant Hubble parameter, one may think of inflation in terms of an effective theory where the de Sitter spacetime symmetry is spontaneously broken down to RW symmetry by the time-evolution of the Hubble rate,  $\dot{H} \neq 0$ . There is then a Goldstone boson,  $\pi$ , associated with the spontaneous breaking of time-translation invariance, which can be used to study model-independent properties of inflation. The Goldstone boson describes a spacetime-dependent shift of the time coordinate, corresponding to an adiabatic

## 26 23. Inflation

perturbation of the matter fields:

$$\delta\phi_i(t, \vec{x}) = \phi_i(t + \pi(t, \vec{x})) - \phi_i(t). \quad (23.88)$$

Thus adiabatic field fluctuations can be absorbed into the spatial metric perturbation,  $\mathcal{R}$  in Eq. (23.28) at first order, in the comoving gauge:

$$\mathcal{R} = -H\pi, \quad (23.89)$$

where we define  $\pi$  on spatially-flat hypersurfaces. In terms of inflaton field fluctuations, we can identify  $\pi \equiv \delta\phi/\dot{\phi}$ , but in principle this analysis is not restricted to inflation driven by scalar fields.

The low-energy effective action for  $\pi$  can be obtained by writing down the most general Lorentz-invariant action and expanding in terms of  $\pi$ . The second-order effective action for the free-field wave modes,  $\pi_k$ , to leading order in slow roll is then

$$S_\pi^{(2)} = - \int d^4x \sqrt{-g} \frac{M_P^2 \dot{H}}{c_s^2} \left[ \dot{\pi}_k^2 - \frac{c_s^2}{R^2} (\nabla\pi)^2 \right], \quad (23.90)$$

where  $\epsilon_H$  is the Hubble slow-roll parameter (Eq. (23.11)). We identify  $c_s^2$  with an effective sound speed, generalising canonical slow-roll inflation, which is recovered in the limit  $c_s^2 \rightarrow 1$ .

The scalar power spectrum on super-Hubble scales (Eq. (23.48)) is enhanced for a reduced sound speed, leading to a reduced tensor-scalar ratio (Eq. (23.49))

$$\mathcal{P}_\zeta(k) \simeq \frac{4\pi}{M_P^2} \frac{1}{c_s^2 \epsilon} \left( \frac{H}{2\pi} \right)_*^2, \quad r \simeq 16(c_s^2 \epsilon)_*. \quad (23.91)$$

At third perturbative order and to lowest order in derivatives, one obtains [91]

$$S_\pi^{(3)} = \int d^4x \sqrt{-g} \frac{M_P^2 (1 - c_s^2) \dot{H}}{c_s^2} \left[ \frac{\dot{\pi} (\nabla\pi)^2}{R^2} - \left( 1 + \frac{2}{3} \frac{\tilde{c}_3}{c_s^2} \right) \dot{\pi}^3 \right]. \quad (23.92)$$

Note that this expression vanishes for canonical fields with  $c_s^2 = 1$ . For  $c_s^2 \neq 1$  the cubic action is determined by the sound speed and an additional parameter  $\tilde{c}_3$ . Both terms in the cubic action give rise to primordial bispectra that are well approximated by equilateral bispectra. However, the shapes are not identical, so one can find a linear combination for which the equilateral bispectra of each term cancel, giving rise to a distinctive orthogonal-type bispectrum [91].

Analysis based on Planck 2015 temperature and polarisation data has placed bounds on several bispectrum shapes including equilateral and orthogonal shapes [90]:

$$f_{\text{NL}}^{\text{equil}} = -4 \pm 43, \quad f_{\text{NL}}^{\text{orthog}} = -26 \pm 21 \quad (68\% \text{ CL}). \quad (23.93)$$

For the simplest case of a constant sound speed, and marginalising over  $\tilde{c}_3$ , this provides a bound on the inflaton sound speed [90]

$$c_s \geq 0.024 \quad (95\% \text{ CL}). \quad (23.94)$$

For a specific model such as DBI inflation [87], corresponding to  $\tilde{c}_3 = 3(1 - c_s^2)/2$ , one obtains a tighter bound [90]:

$$c_s^{DBI} \geq 0.087 \quad (95\% \text{ CL}). \quad (23.95)$$

The Planck team have analysed a wide range of non-Gaussian templates from different inflation models, including tests for deviations from an initial Bunch-Davies vacuum state, direction-dependent non-Gaussianity, and feature models with oscillatory bispectra [90]. No individual feature or resonance is above the three- $\sigma$  significance level after accounting for the look-elsewhere effect. These results are consistent with the simplest canonical, slow-roll inflation models, but do not rule out most alternative models; rather, bounds on primordial non-Gaussianity place important constraints on the parameter space for non-canonical models.

### 23.7.2. Multi-Field Fluctuations :

There is a very large literature on two- and multi-field models of inflation, most of which lies beyond the scope of this review [92]. However, two important general topics merit being mentioned here, namely residual isocurvature perturbations and the possibility of non-Gaussian effects in the primordial perturbations.

One might expect that other scalar fields besides the inflaton might have non-negligible values that evolve and fluctuate in parallel with the inflaton, without necessarily making the dominant contribution to the energy density during the inflationary epoch. However, the energy density in such a field might persist beyond the end of inflation before decaying, at which point it might come to dominate (or at least make a non-negligible contribution to) the total energy density. In such a case, its perturbations could end up generating the density perturbations detected in the CMB. This could occur due to a late-decaying scalar field [88] or a field fluctuation that modulates the end of inflation [93] or the inflaton decay [94].

#### 23.7.2.1. Isocurvature Perturbations:

Primordial perturbations arising in single-field slow-roll inflation are necessarily adiabatic, i.e., they affect the overall density without changing the ratios of different contributions, such as the photon-matter ratio,  $\delta(n_\gamma/n_m)/(n_\gamma/n_m)$ . This is because inflaton perturbations represent a local shift of the time, as described in section Sec. 23.7:

$$\pi = \frac{\delta n_\gamma}{\dot{n}_\gamma} = \frac{\delta n_m}{\dot{n}_m}. \quad (23.96)$$

However, any light scalar field (i.e., one with effective mass less than the Hubble scale) acquires a spectrum of nearly scale-invariant perturbations during inflation. Fluctuations

## 28 23. Inflation

orthogonal to the inflaton in field space are decoupled from the inflaton at Hubble-exit, but can affect the subsequent evolution of the density perturbation. In particular, they can give rise to local variations in the equation of state (non-adiabatic pressure perturbations) that can alter the primordial curvature perturbation  $\zeta$  on super-Hubble scales. Since these fluctuations are statistically independent of the inflaton perturbations at leading order in slow-roll [95], non-adiabatic field fluctuations can only increase the scalar power spectrum with respect to adiabatic perturbations at Hubble exit, while leaving the tensor modes unaffected at first perturbative order. Thus the single-field result for the tensor-scalar ratio (Eq. (23.49)) becomes an inequality [96]

$$r \geq 16\epsilon_* . \quad (23.97)$$

Hence an observational upper bound on the tensor-scalar ratio does not bound the slow-roll parameter  $\epsilon$  in multi-field models.

If all the scalar fields present during inflation eventually decay completely into fully thermalized radiation, these field fluctuations are converted fully into adiabatic perturbations in the primordial plasma [97]. On the other hand, non-adiabatic field fluctuations can also leave behind primordial isocurvature perturbations (Eq. (23.86)) after inflation. In multi-field inflation models it is thus possible for non-adiabatic field fluctuations to generate both curvature and isocurvature perturbations leading to correlated primordial perturbations [98].

The amplitudes of any primordial isocurvature perturbations (Eq. (23.86)) are strongly constrained by the current CMB data, especially on large angular scales. Using temperature and low- $\ell$  polarisation data yields the following bound on the amplitude of cold dark matter isocurvature perturbations at scale  $k = 0.002h^{-1}\text{Mpc}^{-1}$  (marginalising over the correlation angle and in the absence of primordial tensor perturbations) [44]:

$$\frac{\mathcal{P}_{S_m}}{\mathcal{P}_\zeta + \mathcal{P}_{S_m}} < 0.020 \text{ at } 95\% \text{ CL} . \quad (23.98)$$

For fully (anti-)correlated isocurvature perturbations, corresponding to a single isocurvature field providing a source for both the curvature and residual isocurvature perturbations, the bounds become significantly tighter [44]:

$$\frac{\mathcal{P}_{S_m}}{\mathcal{P}_\zeta + \mathcal{P}_{S_m}} < 0.0013 \text{ at } 95\% \text{ CL, correlated} , \quad (23.99)$$

$$\frac{\mathcal{P}_{S_m}}{\mathcal{P}_\zeta + \mathcal{P}_{S_m}} < 0.0008 \text{ at } 95\% \text{ CL, anti - correlated} . \quad (23.100)$$

**23.7.2.2. Local-Type Non-Gaussianity:**

Since non-adiabatic field fluctuations in multi-field inflation may lead to evolution of the primordial curvature perturbation at all orders, it becomes possible to generate significant non-Gaussianity in the primordial curvature perturbation. Non-linear evolution on super-Hubble scales leads to local-type non-Gaussianity, where the local integrated expansion is a non-linear function of the local field values during inflation,  $N(\phi_i)$ . While the field fluctuations at Hubble exit,  $\delta\phi_{i*}$ , are Gaussian in the slow-roll limit, the curvature perturbation,  $\zeta = \delta N$ , becomes a non-Gaussian distribution [99]:

$$\zeta = \sum_i \frac{\partial N}{\partial \phi_i} \delta\phi_i + \frac{1}{2} \sum_{i,j} \frac{\partial^2 N}{\partial \phi_i \partial \phi_j} \delta\phi_i \delta\phi_j + \dots \quad (23.101)$$

with non-vanishing bispectrum in the squeezed limit ( $k_1 \approx k_2 \gg k_3$ ):

$$B_\zeta(k_1, k_2, k_3) \approx \frac{12}{5} f_{\text{NL}}^{\text{local}} \frac{\mathcal{P}_\zeta(k_1)}{4\pi k_1^3} \frac{\mathcal{P}_\zeta(k_3)}{4\pi k_3^3}, \quad (23.102)$$

where

$$\frac{6}{5} f_{\text{NL}}^{\text{local}} = \frac{\sum_{i,j} \frac{\partial^2 N}{\partial \phi_i \partial \phi_j}}{\left(\sum_i \frac{\partial N}{\partial \phi_i}\right)^2}. \quad (23.103)$$

Both equilateral and orthogonal bispectra, discussed above in the context of generalised single field inflation, vanish in the squeezed limit, enabling the three types of non-Gaussianity to be distinguished by observations, in principle.

Non-Gaussianity during multi-field inflation is highly model dependent, though  $f_{\text{NL}}^{\text{local}}$  can often be smaller than unity in multi-field slow-roll inflation [100]. Scenarios where a second light field plays a role during or after inflation can make distinctive predictions for  $f_{\text{NL}}^{\text{local}}$ , such as  $f_{\text{NL}}^{\text{local}} = -5/4$  in some curvaton scenarios [99,101] or  $f_{\text{NL}}^{\text{local}} = 5$  in simple modulated reheating scenarios [94,102]. By contrast the constancy of  $\zeta$  on super-Hubble scales in single-field slow-roll inflation leads to a very small non-Gaussianity [103,104], and in the squeezed limit we have the simple result  $f_{\text{NL}}^{\text{local}} = 5(1 - n_S)/12$  [105,106].

A combined analysis of the Planck temperature and polarization data yields the following range for  $f_{\text{NL}}^{\text{local}}$  defined in (Eq. (23.103)):

$$f_{\text{NL}}^{\text{local}} = 0.8 \pm 5.0 \quad (95\% \text{ CL}). \quad (23.104)$$

This sensitivity is sufficient to rule out parameter regimes giving rise to relatively large non-Gaussianity, but insufficient to probe  $f_{\text{NL}}^{\text{local}} = \mathcal{O}(\epsilon)$ , as expected in single-field models, or the range  $f_{\text{NL}}^{\text{local}} = \mathcal{O}(1)$  found in the simplest two-field models.

Local-type primordial non-Gaussianity can also give rise to a striking scale-dependent bias in the distribution of collapsed dark matter halos and thus the galaxy distribution [107,108]. However, bounds from high-redshift galaxy surveys are not yet competitive with the best CMB constraints.

### 23.8. Pre-Inflation and Anomalies in the CMB

Most work on inflation is done in the context of RW cosmology, which already assumes a high degree of symmetry, or small inhomogeneous perturbations (usually first order) about an RW cosmology. The isotropic RW spacetime is an attractor for many homogeneous, but anisotropic cosmologies in the presence of a false vacuum energy density [109] or a scalar field with suitable self-interaction potential energy [110,111]. However it is much harder to establish the range of highly inhomogeneous initial conditions that yield a successful RW Universe, with only limited studies to date (see, e.g., [112,113,114]).

One of the open questions in inflation is the nature of the pre-inflationary state that should have provided suitable initial conditions for inflation. This would need to have satisfied non-trivial homogeneity and isotropy conditions, and one may ask how these could have arisen and whether there may be some observable signature of the pre-inflationary state. In general, one would expect any such effects to appear at large angular scales, i.e., low multipoles  $\ell$ .

Indeed, various anomalies have been noted in the large-scale CMB anisotropies, also discussed in Chap. 28, “Cosmic Microwave Background” review, including a possible suppression of the quadrupole and other very large-scale anisotropies, an apparent feature in the range  $\ell \approx 20$  to 30, and a possible hemispheric asymmetry. None of these are highly statistically significant in view of the limitations due to cosmic variance [44], and they cannot yet be regarded as signatures of some pre-inflationary dynamics such as string theory or the multiverse. However, is a hot topic for present and future analysis.

### 23.9. Prospects for Future Probes of Inflation

When inflation was first proposed [1,2] there was no evidence for the existence of scalar fields or the accelerated expansion of the universe. The situation has changed dramatically in recent years with the observational evidence that the cosmic expansion is currently accelerating and with the discovery of a scalar particle, namely the Higgs boson (see Chap. 11, “Status of Higgs boson physics” review). These discoveries encourage interest in the idea of primordial accelerated expansion driven by a scalar field, i.e., cosmological inflation. In parallel, successive CMB experiments have been consistent with generic predictions of inflationary models, although without yet providing irrefutable evidence.

Prospective future CMB experiments, both ground- and space-based are reviewed in the separate PDG “Cosmic Microwave Background” review, Chap. 28. The main emphasis in CMB experiments in the coming years will be on ground-based experiments providing improved measurements of  $B$ -mode polarization and greater sensitivity to the tensor-to-scalar ratio  $r$ , and more precise measurements at higher  $\ell$  that will constrain  $n_s$  better. As is apparent from Fig. 23.1 and the discussion of models such as  $R^2$  inflation, there is a strong incentive to reach a  $5\text{-}\sigma$  sensitivity to  $r \sim 3$  to  $4 \times 10^{-3}$ . This could be achieved with a moderately-sized space mission with large sky coverage [115], improvements in de-lensing and foreground measurements. The discussion in Sec. 23.3 (see also Fig. 23.4), also brought out the importance of reducing the uncertainty in

$n_s$ , as a way to constrain post-inflationary reheating and the connection to particle physics. CMB temperature anisotropies probe primordial density perturbations down to comoving scales of order 50 Mpc, beyond which scale secondary sources of anisotropy dominate. CMB spectral distortions could potentially constrain the amplitude and shape of primordial density perturbations on comoving scales from Mpc to kpc due to distortions caused by the Silk damping of pressure waves in the radiation dominated era, before the last scattering of the CMB photons but after the plasma can be fully thermalised [116].

Improved sensitivity to non-Gaussianities is also a priority. In addition to CMB measurements, future large-scale structure surveys will also have roles to play as probes into models of inflation, for which there are excellent prospects. High-redshift galaxy surveys are sensitive to local-type non-Gaussianity due to the scale-dependent bias induced on large scales. Current surveys such as eBOSS, probing out to redshift  $z \sim 2$ , can reach a precision  $\Delta f_{NL} \sim 15$ , from measurements of the galaxy power spectrum, or possibly  $\Delta f_{NL} \sim 10$ , if the galaxy bias can be determined independently [117]. Upcoming surveys such as DESI may reach  $\Delta f_{NL} \sim 4$  [118] comparable with the Planck sensitivity. In the future, radio surveys such as SKA will measure large-scale structure out to redshift  $z \sim 3$  [119], initially through mapping the intensity of the neutral hydrogen 21-cm line, and eventually through radio galaxy surveys which will probe local-type non-Gaussianity to  $f_{NL} \sim 1$ .

Galaxy clustering using DESI and Euclid satellite data could also constrain the running of the scalar tilt to a precision of  $\Delta\alpha_s \approx 0.0028$ , a factor of 2 improvement on Planck constraints, or a precision of 0.0016 using LSST data [118].

The proposed SPHEREx satellite mission [120] will use measurements of the galaxy power spectrum to target a measurement of the running of the scalar spectral index with a sensitivity  $\Delta\alpha_s \sim 10^{-3}$  and local-type primordial non-Gaussianity,  $\Delta f_{NL} \sim 1$ . Including information from the galaxy bispectrum one might reduce the measurement error on non-Gaussianity to  $\Delta f_{NL} \sim 0.2$ , making it possible to distinguish between single-field slow-roll models and alternatives such as the curvaton scenario for the origin of structure, which generate  $f_{NL} \sim 1$ .

## Acknowledgements

The authors are grateful to Vincent Vennin for his careful reading of this manuscript and preparing Fig. 23.3 for this review. The work of J.E. was supported in part by the London Centre for Terauniverse Studies (LCTS), using funding from the European Research Council via the Advanced Investigator Grant 267352 and from the UK STFC via the research grant ST/L000326/1. The work of D.W. was supported in part by the UK STFC research grant ST/K00090X/1.

## References:

1. A.A. Starobinsky, Phys. Lett. **B91**, 99 (1980).
2. A.H. Guth, Phys. Rev. **D23**, 347 (1981).
3. K.A. Olive, Phys. Rept. **190**, 307 (1990).
4. D.H. Lyth and A. Riotto, Phys. Rep. **314**, 1 (1999).

5. A.R. Liddle and D.H. Lyth, *Cosmological inflation and large-scale structure* (Cambridge University Press, 2000).
6. D. Baumann, arXiv:0907.5424 [hep-th].
7. J. Martin, C. Ringeval and V. Vennin, Phys. Dark Univ. **5-6**, 75-235 (2014) [arXiv:1303.3787 [astro-ph.CO]]; J. Martin *et al.*, JCAP **1403** (2014) 039 [arXiv:1312.3529 [astro-ph.CO]]; J. Martin, arXiv:1502.05733 [astro-ph.CO].
8. P.A.R. Ade *et al.* [Planck Collab.], arXiv:1502.01589 [astro-ph.CO].
9. A.H. Guth and E.J. Weinberg, Nucl. Phys. B **212**, 321 (1983).
10. D. La and P.J. Steinhardt, Phys. Rev. Lett. **62**, 376 (1989) [Phys. Rev. Lett. **62**, 1066 (1989)].
11. A.D. Linde, Phys. Lett. **B249**, 18 (1990).
12. F.C. Adams and K. Freese, Phys. Rev. **D43**, 353 (1991) [hep-ph/0504135].
13. A.D. Linde, Phys. Lett. **B108**, 389 (1982).
14. A. Albrecht and P.J. Steinhardt, Phys. Rev. Lett. **48**, 1220 (1982).
15. W.H. Press, Phys. Scr. **21** (1980) 702; S.W. Hawking, Phys. Lett. **115B** (1982) 295; A.A. Starobinsky, Phys. Lett. **117B** (1982) 175; A.H. Guth and S.Y. Pi, Phys. Rev. Lett. **49** (1982) 1110.
16. J.M. Bardeen, P.J. Steinhardt and M.S. Turner, Phys. Rev. **D28**, 679 (1983).
17. V.F. Mukhanov and G.V. Chibisov, JETP Lett. **33** (1981) 532.
18. K.S. Stelle, Gen. Rel. Grav. **9** (1978) 353.
19. B. Whitt, Phys. Lett. **B145**, 176 (1984).
20. D. Wands, Class. Quant. Grav. **11**, 269 (1994) [gr-qc/9307034].
21. S.R. Coleman and F. De Luccia, Phys. Rev. **D21**, 3305 (1980).
22. M. Sasaki *et al.*, Phys. Lett. **B317**, 510 (1993).
23. M. Bucher, A.S. Goldhaber and N. Turok, Phys. Rev. **D52**, 3314 (1995) [hep-ph/9411206].
24. A.D. Linde and A. Mezhlumian, Phys. Rev. **D52**, 6789 (1995) [astro-ph/9506017].
25. A.R. Liddle, P. Parsons and J.D. Barrow, Phys. Rev. **D50**, 7222 (1994) [astro-ph/9408015].
26. L. Kofman, A.D. Linde and A.A. Starobinsky, Phys. Rev. **D56**, 3258 (1997) [hep-ph/9704452].
27. B.A. Bassett, S. Tsujikawa and D. Wands, Rev. Mod. Phys. **78**, 537 (2006) [astro-ph/0507632].
28. A.D. Linde, Phys. Rev. **D49**, 748 (1994) [astro-ph/9307002].
29. A.D. Dolgov and A.D. Linde, Phys. Lett. **B116**, 329 (1982).
30. J.R. Ellis *et al.*, Nucl. Phys. B **238**, 453 (1984).
31. M. Kawasaki and T. Moroi, Prog. Theor. Phys. **93**, 879 (1995) [hep-ph/9403364, hep-ph/9403061].
32. J.H. Traschen and R.H. Brandenberger, Phys. Rev. **D42**, 2491 (1990).
33. G.V. Chibisov and V.F. Mukhanov, Mon. Not. Roy. Astron. Soc. **200**, 535 (1982).
34. H. Kodama and M. Sasaki, Prog. Theor. Phys. Suppl. **78**, 1 (1984).
35. V.F. Mukhanov, H.A. Feldman and R.H. Brandenberger, Phys. Rept. **215**, 203 (1992).
36. K.A. Malik and D. Wands, Phys. Rept. **475**, 1 (2009) [arXiv:0809.4944 [astro-ph]].

37. M. Sasaki, Prog. Theor. Phys. **76**, 1036 (1986) V.F. Mukhanov, Sov. Phys. JETP **67**, 1297 (1988) [Zh. Eksp. Teor. Fiz. **94N7**, 1 (1988)].
38. A.A. Starobinsky, JETP Lett. **30**, 682 (1979) [Pisma Zh. Eksp. Teor. Fiz. **30**, 719 (1979)].
39. E.D. Stewart and D.H. Lyth, Phys. Lett. **B302**, 171 (1993) [gr-qc/9302019].
40. D. Wands *et al.*, Phys. Rev. **D62**, 043527 (2000) [astro-ph/0003278].
41. A.R. Liddle and S.M. Leach, Phys. Rev. **D68**, 103503 (2003) [astro-ph/0305263].
42. P.A.R. Ade *et al.* [BICEP2/Keck and Planck Collabs.], Phys. Rev. Lett. **114**, 101301 (2015) [arXiv:1502.00612 [astro-ph.CO]]; P.A.R. Ade *et al.* [BICEP2 and Keck Array Collabs.], Phys. Rev. Lett. **116**, 031302 (2016) [arXiv:1510.09217 [astro-ph.CO]].
43. S.M. Leach, A.R. Liddle, J. Martin, and D.J. Schwarz, Phys. Rev. **D66**, 23515 (2002).
44. P.A.R. Ade *et al.* [Planck Collab.], arXiv:1502.02114 [astro-ph.CO].
45. D. Kazanas, Astrophys. J. **241** (1980) L59.
46. K. Sato, Mon. Not. Roy. Astron. Soc. **195**, 467 (1981).
47. A. Billoire and K. Tamvakis, Nucl. Phys. B **200** (1982) 329; J.D. Breit, S. Gupta and A. Zaks, Phys. Rev. Lett. **51**, 1007 (1983).
48. A.D. Linde, Phys. Lett. **B129**, 177 (1983).
49. D.V. Nanopoulos, K.A. Olive and M. Srednicki, Phys. Lett. **B127**, 30 (1983).
50. J. Ellis, D.V. Nanopoulos and K.A. Olive, Phys. Rev. Lett. **111**, 111301 (2013) [Phys. Rev. Lett. **111**, 129902 (2013)] [arXiv:1305.1247 [hep-th]].
51. C. Pallis and Q. Shafi, JCAP **1503** (2015) 03, 023 [arXiv:1412.3757 [hep-ph]].
52. L. Boubekeur and D.H. Lyth, JCAP **0507** (2005) 010 [hep-ph/0502047].
53. G.R. Dvali, Q. Shafi and S. Solganik, hep-th/0105203; J. Garcia-Bellido, R. Rabadan and F. Zamora, JHEP **0201** (2002) 036 [hep-th/0112147]; S. Kachru *et al.*, JCAP **0310** (2003) 013 [hep-th/0308055].
54. K. Freese, J.A. Frieman and A.V. Olinto, Phys. Rev. Lett. **65**, 3233 (1990) F.C. Adams *et al.*, Phys. Rev. **D47**, 426 (1993) [hep-ph/9207245].
55. For a recent review of axion inflation, see E. Pajer and M. Peloso, Class. Quant. Grav. **30** (2013) 214002 [arXiv:1305.3557 [hep-th]].
56. E. Silverstein and A. Westphal, Phys. Rev. **D78**, 106003 (2008) [arXiv:0803.3085 [hep-th]].
57. L. McAllister, E. Silverstein and A. Westphal, Phys. Rev. **D82**, 046003 (2010) [arXiv:0808.0706 [hep-th]].
58. F.L. Bezrukov and M. Shaposhnikov, Phys. Lett. **B659**, 703 (2008) [arXiv:0710.3755 [hep-th]].
59. D. Buttazzo *et al.*, JHEP **1312** (2013) 089 [arXiv:1307.3536 [hep-ph]].
60. H.P. Nilles, Phys. Rept. **110** (1984) 1; H.E. Haber and G.L. Kane, Phys. Rept. **117** (1985) 75.
61. J.R. Ellis *et al.*, Phys. Lett. **B118**, 336 (1982).
62. N. Okada and Q. Shafi, arXiv:1311.0921 [hep-ph].
63. H. Murayama *et al.*, Phys. Rev. Lett. **70**, 1912 (1993).

64. J. Ellis, M. Fairbairn and M. Sueiro, JCAP **1402** (2014) 044 [arXiv:1312.1353 [astro-ph.CO]].
65. D. Croon, J. Ellis and N.E. Mavromatos, Phys. Lett. **B724**, 165 (2013) [arXiv:1303.6253 [astro-ph.CO]].
66. G.R. Dvali, Q. Shafi and R.K. Schaefer, Phys. Rev. Lett. **73**, 1886 (1994) [hep-ph/9406319].
67. D.V. Nanopoulos *et al.*, Phys. Lett. **B123**, 41 (1983).
68. A.B. Goncharov and A.D. Linde, Phys. Lett. **B139**, 27 (1984).
69. E. Cremmer *et al.*, Nucl. Phys. B **212** (1983) 413.
70. R. Holman, P. Ramond and G.G. Ross, Phys. Lett. **B137**, 343 (1984).
71. E.J. Copeland *et al.*, Phys. Rev. **D49**, 6410 (1994) [astro-ph/9401011]; E.D. Stewart, Phys. Rev. **D51**, 6847 (1995) [hep-ph/9405389].
72. G.D. Coughlan *et al.*, Phys. Lett. B **131**, 59 (1983); A.S. Goncharov, A.D. Linde and M.I. Vysotsky, Phys. Lett. **B147**, 279 (1984); T. Banks, D.B. Kaplan and A.E. Nelson, Phys. Rev. **D49**, 779 (1994) [hep-ph/9308292]; B. De Carlos *et al.*, Phys. Lett. **B318**, 447 (1993) [hep-ph/9308325]; M. Kawasaki, T. Moroi and T. Yanagida Phys. Lett. **B370**, 52 (1996) [hep-ph/9509399].
73. J. Ellis, D.V. Nanopoulos, and M. Quiros, Phys. Lett. **B174**, 176 (1986).
74. T. Moroi, M. Yamaguchi and T. Yanagida Phys. Lett. **B342**, 105 (1995) [hep-ph/9409367].
75. M. Kawasaki, M. Yamaguchi and T. Yanagida, Phys. Rev. Lett. **85**, 3572 (2000) [hep-ph/0004243]; K. Nakayama, F. Takahashi and T.T. Yanagida, JCAP **1308** (2013) 038 [arXiv:1305.5099 [hep-ph]].
76. E. Cremmer *et al.*, Phys. Lett. **B133**, 61 (1983).
77. For some older examples of no-scale inflationary models see, e.g., A.S. Goncharov and A.D. Linde, Class. Quant. Grav. **1**, L75 (1984); C. Kounnas and M. Quiros, Phys. Lett. **B151**, 189 (1985); J.R. Ellis *et al.*, Phys. Lett. **B152**, 175 (1985) [Erratum-ibid. **156B** (1985) 452].
78. J.R. Ellis, C. Kounnas and D.V. Nanopoulos, Nucl. Phys. B **247** (1984) 373.
79. E. Witten, Phys. Lett. **B155**, 151 (1985).
80. J. Ellis, D.V. Nanopoulos and K.A. Olive, JCAP **1310** (2013) 009 [arXiv:1307.3537].
81. For a recent review and more references, see J. Ellis *et al.*, arXiv:1507.02308 [hep-ph].
82. R. Kallosh, A. Linde and D. Roest, JHEP **1311** (2013) 198 [arXiv:1311.0472].
83. A.R. Liddle, Mon. Not. Roy. Astron. Soc. **377**, L74 (2007) [astro-ph/0701113].
84. J. Martin, C. Ringeval and V. Vennin, arXiv:1603.02606 [astro-ph.CO] We thank Vincent Vennin for providing the adapted version of Fig. 3 from this reference.
85. J. Ellis *et al.*, JCAP **1507** (2015) 07, 050 [arXiv:1505.06986 [hep-ph]].
86. C. Armendariz-Picon, T. Damour and V.F. Mukhanov, Phys. Lett. **B458**, 209 (1999) [hep-th/9904075].
87. M. Alishahiha, E. Silverstein and D. Tong, Phys. Rev. **D70**, 123505 (2004) [hep-th/0404084].
88. K. Enqvist and M.S. Sloth, Nucl. Phys. B **626** (2002) 395 [hep-ph/0109214]; D.H. Lyth and D. Wands, Phys. Lett. **B524**, 5 (2002) [hep-ph/0110002]; T. Moroi

- and T. Takahashi, Phys. Lett. **B522**, 215 (2001) [Phys. Lett. **B539**, 303 (2002)] [hep-ph/0110096].
89. N. Bartolo *et al.*, Phys. Rept. **402**, 103 (2004) [astro-ph/0406398].
  90. P.A.R. Ade *et al.* [Planck Collab.], arXiv:1502.01592 [astro-ph.CO].
  91. L. Senatore, K.M. Smith and M. Zaldarriaga, JCAP **1001**, 028 (2010) [arXiv:0905.3746 [astro-ph.CO]].
  92. See, for example, C. Gordon *et al.*, Phys. Rev. **D63**, 023506 (2001) [astro-ph/0009131]; C.T. Byrnes and D. Wands, Phys. Rev. **D74**, 043529 (2006) [astro-ph/0605679]; R. Easther *et al.*, Phys. Rev. Lett. **112**, 161302 (2014) [arXiv:1312.4035 [astro-ph.CO]]; J. Ellis *et al.*, JCAP **1501** (2015) 01, 010 [arXiv:1409.8197 [hep-ph]]; S. Renaux-Petel and K. Turzynski, JCAP **1506** (2015) 06, 010 [arXiv:1405.6195 [astro-ph.CO]].
  93. D.H. Lyth, JCAP **0511**, 006 (2005) [astro-ph/0510443].
  94. G. Dvali, A. Gruzinov and M. Zaldarriaga, Phys. Rev. **D69**, 023505 (2004) [astro-ph/0303591].
  95. C.T. Byrnes and D. Wands, Phys. Rev. **D74**, 043529 (2006) [astro-ph/0605679].
  96. D. Wands *et al.*, Phys. Rev. **D66**, 043520 (2002) [astro-ph/0205253].
  97. S. Weinberg, Phys. Rev. **D67**, 123504 (2003) [astro-ph/0302326].
  98. D. Langlois, Phys. Rev. **D59**, 123512 (1999) [astro-ph/9906080].
  99. D.H. Lyth and Y. Rodriguez, Phys. Rev. Lett. **95**, 121302 (2005) [astro-ph/0504045].
  100. F. Vernizzi and D. Wands, JCAP **0605**, 019 (2006) [astro-ph/0603799].
  101. M. Sasaki, J. Valiviita and D. Wands, Phys. Rev. **D74**, 103003 (2006) [astro-ph/0607627].
  102. G. Dvali, A. Gruzinov and M. Zaldarriaga, Phys. Rev. **D69**, 083505 (2004) [astro-ph/0305548].
  103. D.S. Salopek and J.R. Bond, Phys. Rev. **D43**, 1005 (1991).
  104. A. Gangui *et al.*, Astrophys. J. **430**, 447 (1994) [astro-ph/9312033].
  105. J.M. Maldacena, JHEP **0305**, 013 (2003) [astro-ph/0210603].
  106. V. Acquaviva *et al.*, Nucl. Phys. B **667**, 119 (2003) [astro-ph/0209156].
  107. N. Dalal *et al.*, Phys. Rev. **D77**, 123514 (2008) [arXiv:0710.4560 [astro-ph]].
  108. S. Matarrese and L. Verde, Astrophys. J. **677**, L77 (2008) [arXiv:0801.4826 [astro-ph]].
  109. R.M. Wald, Phys. Rev. **D28**, 2118 (1983).
  110. M. Heusler, Phys. Lett. **B253**, 33 (1991).
  111. Y. Kitada and K.-i. Maeda, Phys. Rev. **D45**, 1416 (1992).
  112. D.S. Goldwirth and T. Piran, Phys. Rept. **214**, 223 (1992).
  113. T. Vachaspati and M. Trodden, Phys. Rev. **D61**, 023502 (1999) [gr-qc/9811037].
  114. W.E. East *et al.*, arXiv:1511.05143 [hep-th].
  115. Proposed space missions include PIXIE: A. Kogut *et al.*, JCAP **1107** (2011) 025 [arXiv:1105.2044 [astro-ph.CO]]; LiteBird: <http://litebird.jp/eng/> and Cosmic Origins Explorer (COre): <http://www.core-mission.org>.
  116. J. Chluba, J. Hamann and S.P. Patil, Int. J. Mod. Phys. D **24**, no. 10, 1530023 (2015) [arXiv:1505.01834 [astro-ph.CO]].

## 36 *23. Inflation*

117. G.B. Zhao *et al.*, Mon. Not. Roy. Astron. Soc. **457**, 2377 (2016) [arXiv:1510.08216 [astro-ph.CO]].
118. A. Font-Ribera *et al.*, JCAP **1405**, 023 (2014) [arXiv:1308.4164 [astro-ph.CO]].
119. R. Maartens *et al.* [SKA Cosmology SWG Collab.], PoS AASKA **14**, 016 (2015) [arXiv:1501.04076 [astro-ph.CO]].
120. O. Dor *et al.*, arXiv:1412.4872 [astro-ph.CO].